Australian Government

Department of Defence
Defence Science and
Technology Group

Measurement of Surface Strains from a Composite Hydrofoil using Fibre Bragg Grating Sensing Arrays

Claire Davis*, Patrick Norman*, Andrew Phillips# and Asintha Nanayakkara#

Aerospace Division*, Maritime Division#
Defence Science and Technology Group

DST-Group-TN-1438

ABSTRACT

This report details a methodology for the permanent attachment of fibre optic strain gauge (Bragg grating) arrays to the surface of a composite hydrofoil and reports on an experiment to measure surface strains from the hydrofoil under static and fatigue loading conditions. The strain data from the optical gauges is compared to measurements from electrical resistance strain gauges nearby and to model predictions and an assessment is made on the suitability of this technique for strain-mapping in a service environment.

RELEASE LIMITATION

Approved for public release

APPROVED FOR PUBLIC RELEASE

Measurement of Surface Strains from a Composite Hydrofoil using Fibre Bragg Grating Sensing Arrays

Executive Summary

The Advanced Material Propeller (AMP) Project will demonstrate the potential capability gains from a composite submarine propeller. The project will be delivered through a collaborative agreement between Australia, represented by the RAN, DMO and DST Group, and the United States Department of Defense (DoD). The project will involve the design and manufacture of a composite propeller including test articles (hubs and blades), structural fatigue testing, propeller certification, a limited full-scale at-sea trial of a composite propeller on board a Collins Class Submarine (CCSM).

As part of the lead-in activities associated with this project a large-scale unclassified composite hydrofoil of a scale comparable to the AMP test articles was manufactured to assist with preparation for the main structural fatigue testing program. The hydrofoil was designed to contain many of the important features of the AMP test articles such as hydrodynamic profile and thickness and width tapers. The hydrofoil was manufactured at DST group and tested in the same structural test assembly as will be used to test the AMP test articles.

This report details part of the hydrofoil test where a network of optical fibre Bragg grating (FBG) sensing arrays was applied to the surface of the composite hydrofoil for the measurement of surface strains during full-scale structural testing. The strain data from the optical gauges was compared to electrical resistance strain gauges mounted nearby and to model predictions.

The results show that FBG arrays may be surface-mounted with minimal intrusion to a large composite structure and used to provide detailed strain distribution information from across the surface. However the thermal-cure adhesive used to attach the sensors to the part introduced a strain gradient in the sensor in regions where there was a significant thickness variation in the structure and hence should be used with caution on composite parts where there is a large change in cross-sectional thickness.

This page is intentionally blank

Contents

Abbreviations

AMP	Advanced Material Propeller
CCSM	Collins Class Submarine
DMO	Defence Materiel Organisation
DoD	Department of Defense (U.S.)
DST Group	Defence Science and Technology
FBG	Fibre Bragg Grating
FEA	Finite Element Analysis
FSG	Foil Strain Gauge
IPA	Iso Propyl Alcohol
RAN	Royal Australian Navy
RTM	Resin Transfer Moulding

1. Introduction

The Advanced Material Propeller (AMP) project is a joint Australian/U.S. collaborative research program to demonstrate the potential capability gains from a composite submarine propeller. The project comprises several elements: the design and manufacture of a composite propeller including test articles (hubs and blades), structural fatigue testing, propeller certification, a limited full-scale sea trial of a composite propeller on board a Collins Class Submarine (CCSM) and data collection, analysis and reporting.

As part of the lead-in activities associated with this project a large composite hydrofoil, as shown in Figure 1, was fabricated at the DST Group to serve as an unclassified representative test article upon which to develop experimental, analytical and non-destructive evaluation techniques prior to their application on the composite propeller [1].
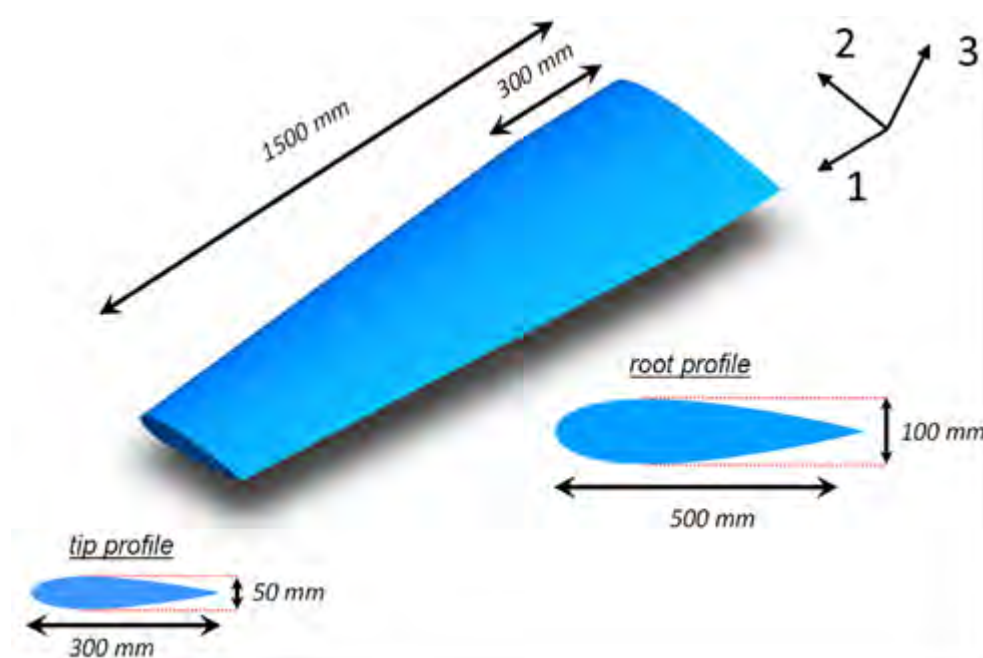

Figure 1: Schematic diagram showing the profile and main dimensions of the generic composite hydrofoil.

One element of the hydrofoil test program was to demonstrate permanent installation of a network of fibre optic Bragg grating strain sensors to the surface of a thick curved composite part. There were several objectives under investigation in this part of the work:

- Validation of the fibre optic sensor attachment process on a large, thick curved composite part.

- Validation of the strain measurements by comparison with strain data from a finite element (FE) model and with nearby electrical resistance strain gauges.

- Confirmation of the reliability and durability of the sensors and adhesive packaging under fatigue loading.

- Development of techniques for dynamic visualisation of strain distributions from a network of sensing points.

This report provides an overview of the attachment process utilised for the fibre optic sensing arrays and the instrumentation used to interrogate the sensors. The strain data is reported under different loading conditions and compared with measurements from nearby electrical resistance foil gauges and with FE model data. Finally some analysis of the data is given along with commentary about the suitability of this strain measurement technique and the packaging process for the proposed sea trial.

2. Background

A Fibre Bragg Grating (FBG) is a periodic change of the optical refractive index written into the core of an optical fibre [2]. The periodic modulation is achieved by exposing the fibre (side-on) to interference fringes from an ultra-violet laser beam. The region of the optical fibre exposed to the beam is altered via modification of the oxygen vacancy-defect absorption band resulting in a small increase in the refractive index. FBGs typically reflect light over a narrow wavelength range and transmit all other wavelengths.
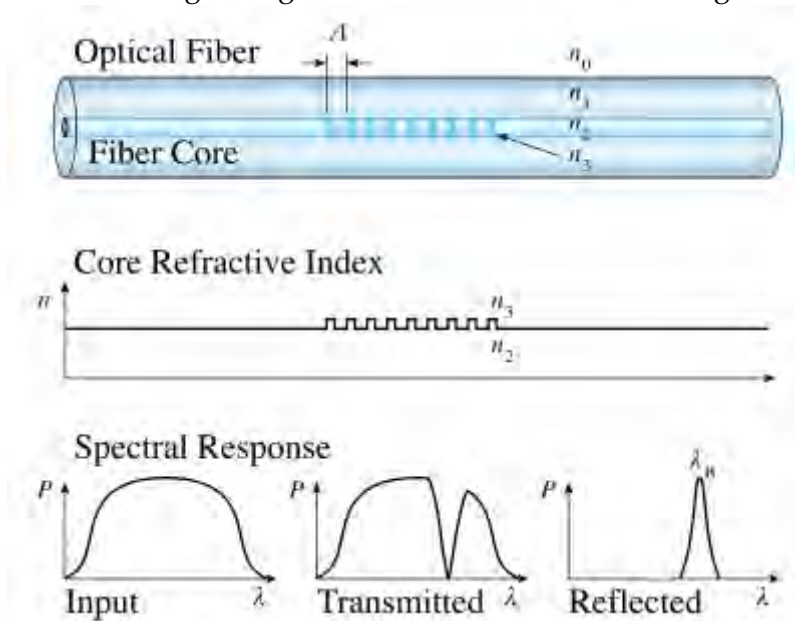

Figure 2: FBG periodic structure in optical fibre core, with refractive index profile and spectral response.

The relationship between the reflected wavelength λ_{Bragg} and the period of the refractive index change can be approximated by the following equation:

$$\lambda_{\mathrm{Bragg}} = 2n_{\mathrm{eff}} \, \Lambda \qquad\qquad (1)$$

where n_{eff} is the effective refractive index of the fiber, and Λ is the period of the grating. Uniform changes in the axial strain and/or temperature in the region of the grating will alter the period of the index modulation and thus result in a shift in the reflected Bragg wavelength [3]. By monitoring the change in reflected wavelength peak, λ_{Bragg}, FBGs may be used as temperature and/or strain sensors. Multiple spectrally encoded gratings may be written at different points along the fibre to allow spatially separated measurements of strain as shown schematically in Figure 3.
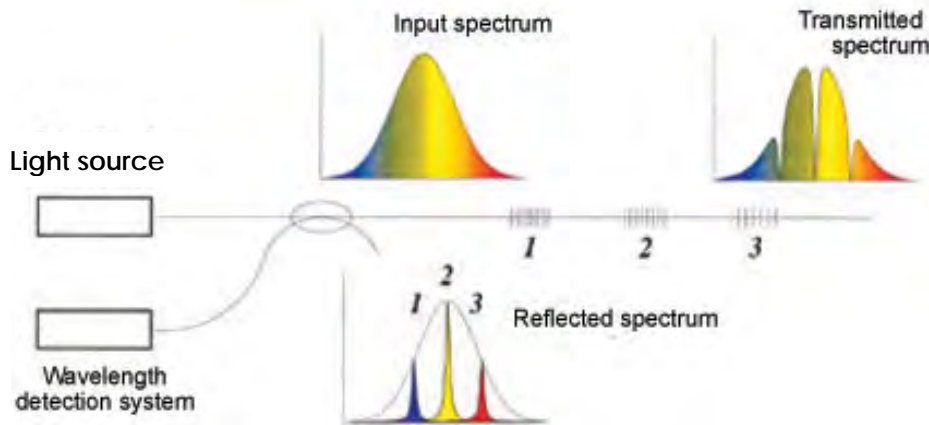

Figure 3: Principle of wavelength based multiplexing using spectrally separated FBGs.

There are many practical advantages to using Bragg gratings as an alternative to conventional electrical resistance foil gauges as outlined below:

- FBGS are small, lightweight and can be surface-mounted or embedded with minimal intrusion on the host structure.

- FBGs are intrinsically passive (no electrical power necessary) and therefore the signal is immune to electromagnetic interference and the sensing network is insensitive to moisture ingress. In addition they can be used can be used in high-voltage or electrically sensitive environments.

- FBGs written during the fibre draw process can measure and endure very high strains (> 1% or 10000 µstrain for long-term measurements and 5% or 50000 µstrain for short-term measurements) [4].

- FBGs are constructed in glass and hence are inherently corrosion resistant.

- Multiple sensors can be written in a single optical fibre reducing the requirement for complex routing of wires and multiple connectors in regions where detailed strain information is required.

- Strain measurements using FBGs are absolute, do not require recalibration or zeroing and exhibit excellent long-term stability.

For the proposed submarine propeller trial, distributed strain information will be required from across the propeller blade surface in order to fully characterise its performance in the service environment. The strain sensors will be required to be integrated onto the blade with minimal intrusion on the hydrodynamic profile and the signals from each sensor will need to be routed via the propeller hub into an instrumentation pod housed within a tail-cone attached to the rear of the propeller.

The capacity for distributed sensing provided by FBGs mean that the number of connections between the sensors and the instrumentation pod can be significantly reduced when compared to electrical resistance foil strain gauges (FSGs) which require three isolated electrical connections per sensing point. In addition the physical size of optical fibres (approximately 250 μm in diameter) means that they can be retro-fitted relatively easily onto the propeller blades without significantly affecting their surface profile. These will be significant advantages in the proposed trial environment which presents many engineering challenges. Accordingly, the development of techniques for the reliable attachment and measurement of surface strains using FBG sensing arrays was one of the primary objectives of the hydrofoil test program in preparation for a CCSM propeller trial.

3. Preparation of the Test Article

3.1 Test Article Fabrication

The composite hydrofoil used for the test article was manufactured using a closed mould resin transfer moulding (RTM) process in a custom-built Aluminium mould. The matrix material was the low viscosity Kinetix R118 resin used in conjunction with the long pot life H103 hardener (supplied by ATL Composites). The foil was produced in two halves and then subsequently adhesively bonded together with Techniglue-HP R15 (supplied by ATL Composites). The core section of the foil was made from a heavy weight 1430 g/m^2 E-glass quadraxial fabric with a light chopped strand mat backing (Glass-Quad). The outer skin was made from a quasi-isotropic layup of 48K 500 g/m² unidirectional Carbon (Carbon-500UD) and 400 g/m² 12k carbon double bias ±45 (Carbon-DB) layers. High permeability sandwich mat layers (Glass-Mat) were included at several places to improve resin distribution through the skin and a lightweight E-glass basketweave (Glass-Basket) was included as the outer ply to improve surface finish. A photograph of the completed foil is shown in Figure 4.

Figure 4: Completed Carbon/fibreglass composite hydrofoil prior to instrumentation.

3.2 Fibre Optic Sensing Locations

The sensing locations were chosen to measure strain in regions where high strains or strain gradients were predicted by the FE modelling. Four optical fibres each containing 12 FBG sensors spatially separated by 80 mm were bonded to the top surface of the foil running span wise as shown schematically in Figure 5.
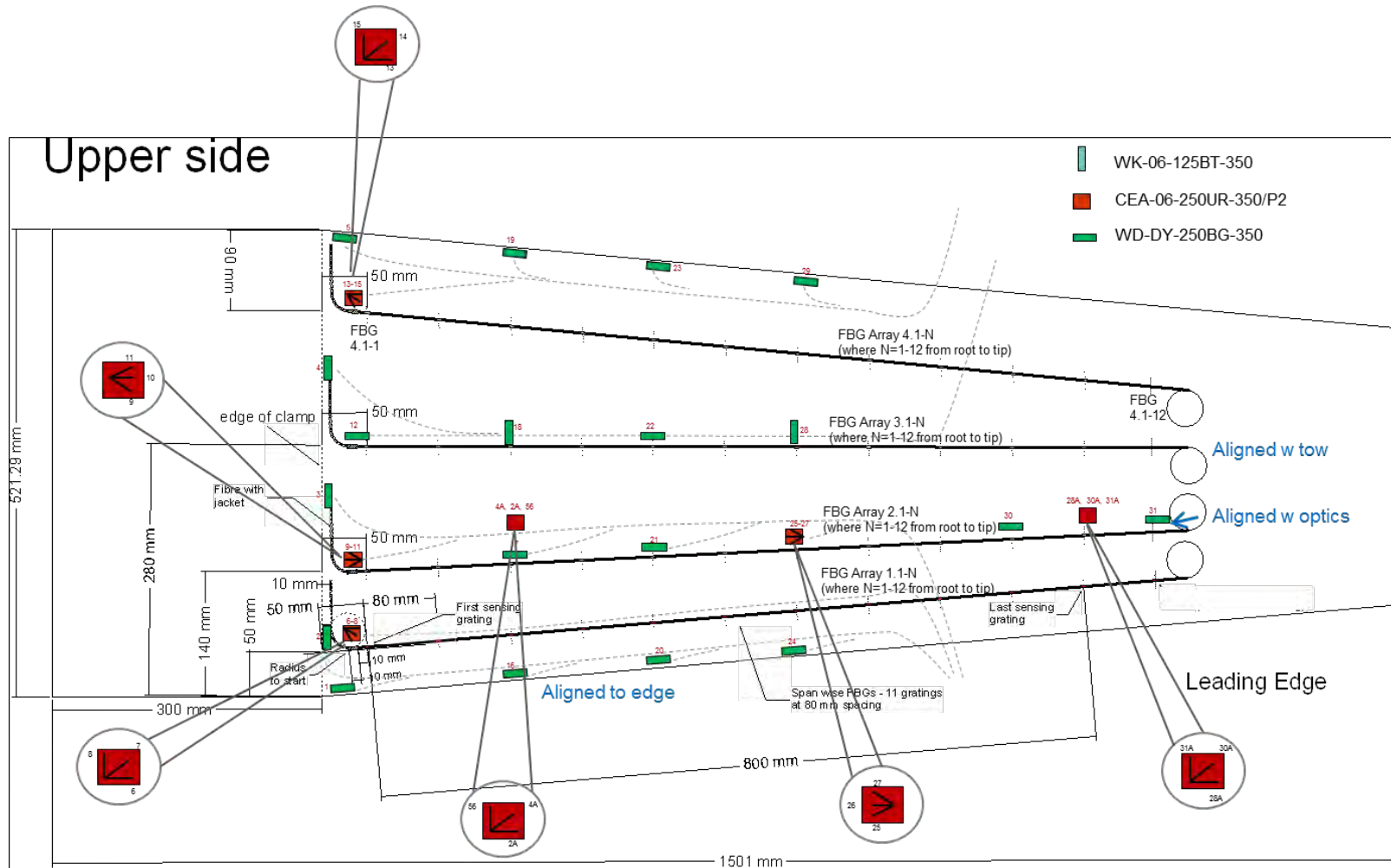
Figure 5: Schematic drawing of the upper surface of the hydrofoil showing the location of the foil strain gauges, fibre optic Bragg grating sensors and their associated wiring.

An additional 4 fibres were bonded chord wise to the bottom surface of the foil. For the chord wise sensors the two fibres closest to the root contained 10 FBGs spatially separated by 50 mm, the two fibres further away from the root where the part narrows contained 9 FBG sensors also with a 50 mm separation as shown in Figure 6.
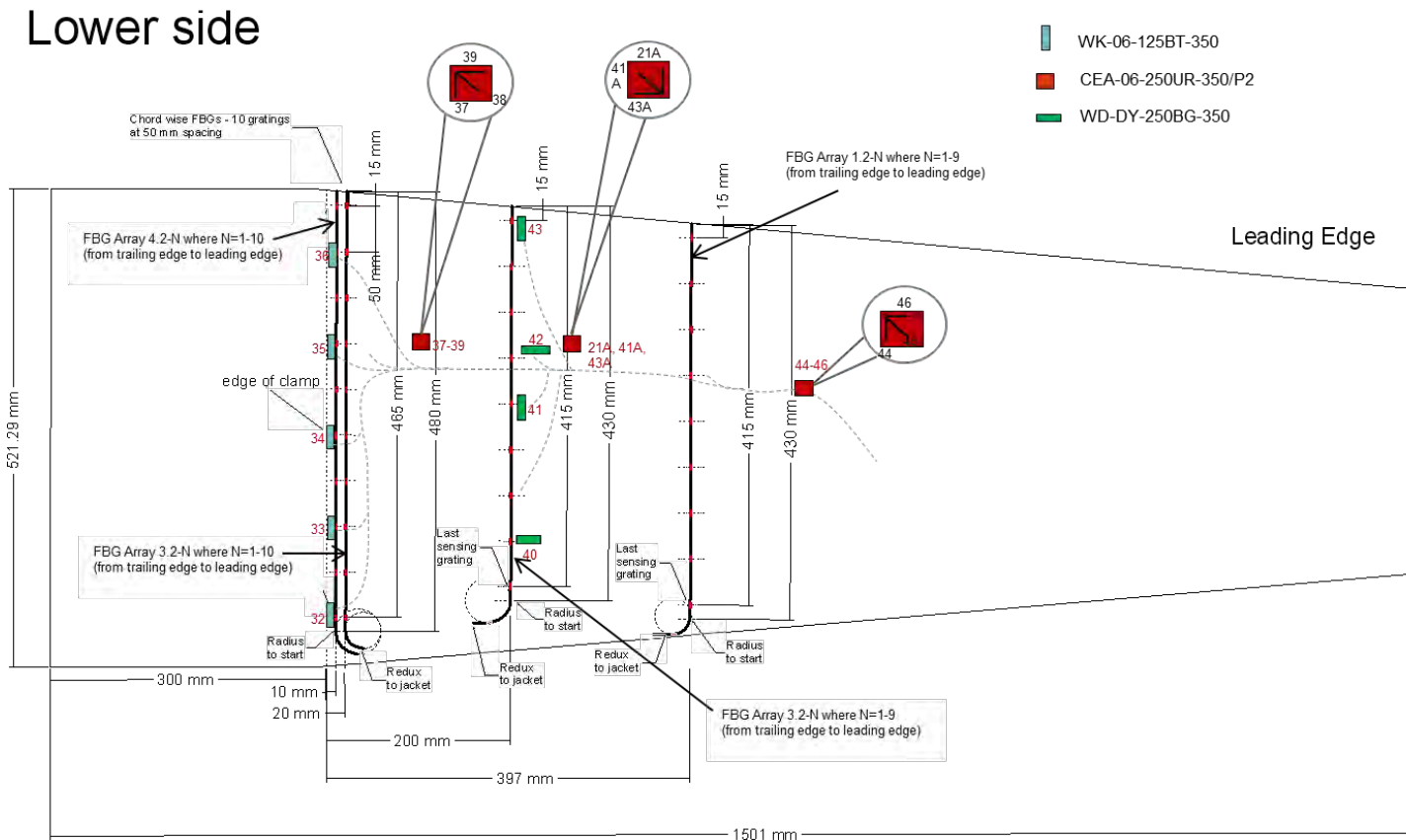

Figure 6: Schematic drawing of the lower surface of the hydrofoil showing the location of the foil strain gauges, fibre optic Bragg grating sensors and their associated wiring.

3.3 Electrical Foil Gauge Sensing Locations

The strain from 56 foil strain gauges located on the top and bottom surfaces of the generic hydrofoil was also measured. Three types of gauges were installed; WD-DY-250BG-350 a single general purpose gauge with a resistance of 350 Ω and a gauge factor of 3.29, WK-06-125BT-350 a smaller single purpose gauge with a resistance of 350 Ω and a gauge factor of 2.06 and CAE-06-250UR-350P2 a wired general purpose rectangular rosette with three 45° elements, a resistance of 350 Ω and a gauge factor of 2.105. These gauges were strategically applied in the regions thought to experience the most strain under static and fatigue loading as indicated in Figures 5 and 6 using a standard surface preparation [5] and application technique [6,7].

3.4 Fibre Optic Sensor Attachment Process

The proposed methodology for surface mounting of the optical fibre sensing arrays to the part involves the use of a heat-activated film adhesive (Redux 312) [8,9]. The optical fibres were laid into channels formed on the part surface using tape and then overlaid with strips of the adhesive film. The channels were then vacuum bagged and thermally cured. The details of this process are described in the proceeding sections.

3.4.1 Surface Preparation

In the areas where the sensing fibres were to be attached, the surface was cleaned with iso-propyl alcohol (IPA) and lightly abraded using a fine grade abrasive paper. After abrading any abrasive by-product was removed using clean compressed air. The adhesive channel and strain sensing locations were then marked out. Three layers of flash breaker tape (Flash breaker® 5) were used to form the channel walls into which the film adhesive was laid as shown in Figure 7.

Figure 7: Photo showing the adhesive channels on top side of test article.

3.4.2 Sensor Lay-up

After preparation of the channels the next stage was to pre-tension the optical fibre along the centre of the channel with the sensor locations aligned with the markings on the channel tape and the fibre lying flat along the surface of the part. The fibres were fixed using flash breaker tape to hold the tension during cure. The buffer jacket over the optical fibre was sealed with vacuum sealant tape to prevent resin run-out between and the fibre and the buffer during the cure process.
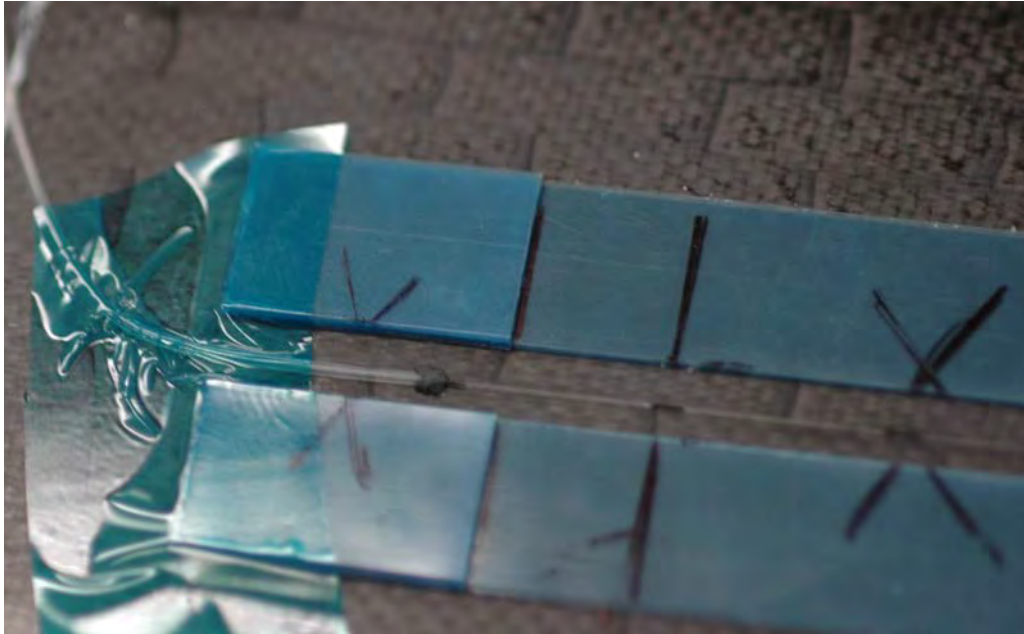

Figure 8: Photo showing the sensing fibre laid up in channel prior to application of film adhesive.

3.4.3 Adhesive Film Lay-up

The Redux film was removed from the freezer and allowed to come to room temperature. Any excess at the edges of the film where there is a non-uniform distribution of resin (as shown in figure 9) was trimmed.

Figure 9: Example of non-uniform distribution of resin on carrier tape at the edge of the roll.

A cutting template with the same dimensions as the channel width is used to cut strips of the Redux with the protective layers still in place on both the top and bottom of the material as shown in Figure 10. Shorter additional sections of Redux film are used to build up the channel height to incorporate the buffer jacket at the end of each channel.
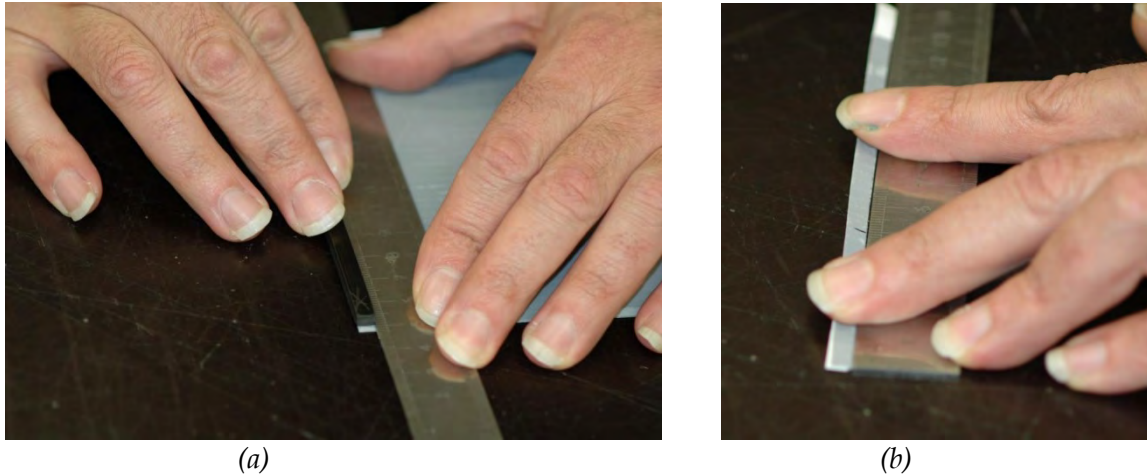

(a)	*(b)*

Figure 10: Photos showing the cutting of Redux strips to match channel width using cutting template.

The bottom layer of the protective film was removed from the Redux strips and then placed in the channel with tweezers and the tape is pressed into the channels using a narrow Teflon spatula.

After all the film adhesive strips have been laid up in the channels a thin roll of vacuum sealant tape was placed along the end of each channel extending across the channel walls and pressed down into the channels as shown in Figures 11 and 12. Sealant tape was also used along the channel edges in the built up regions of channel to prevent run-out of excess resin during the cure process.
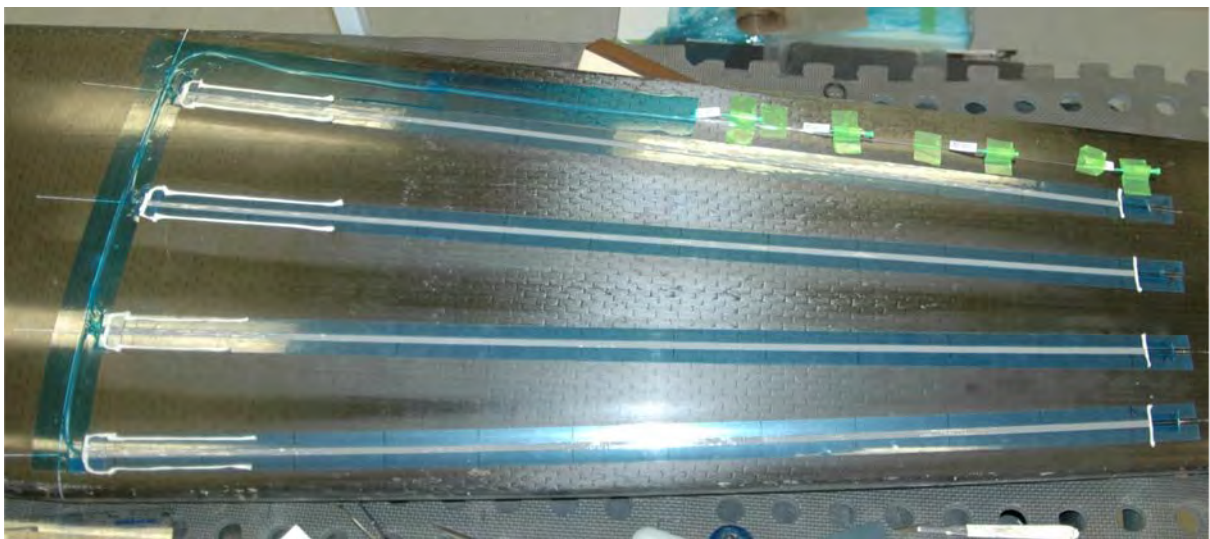

Figure 11: Photo showing the sealing of the span wise channels using vacuum sealant tape.
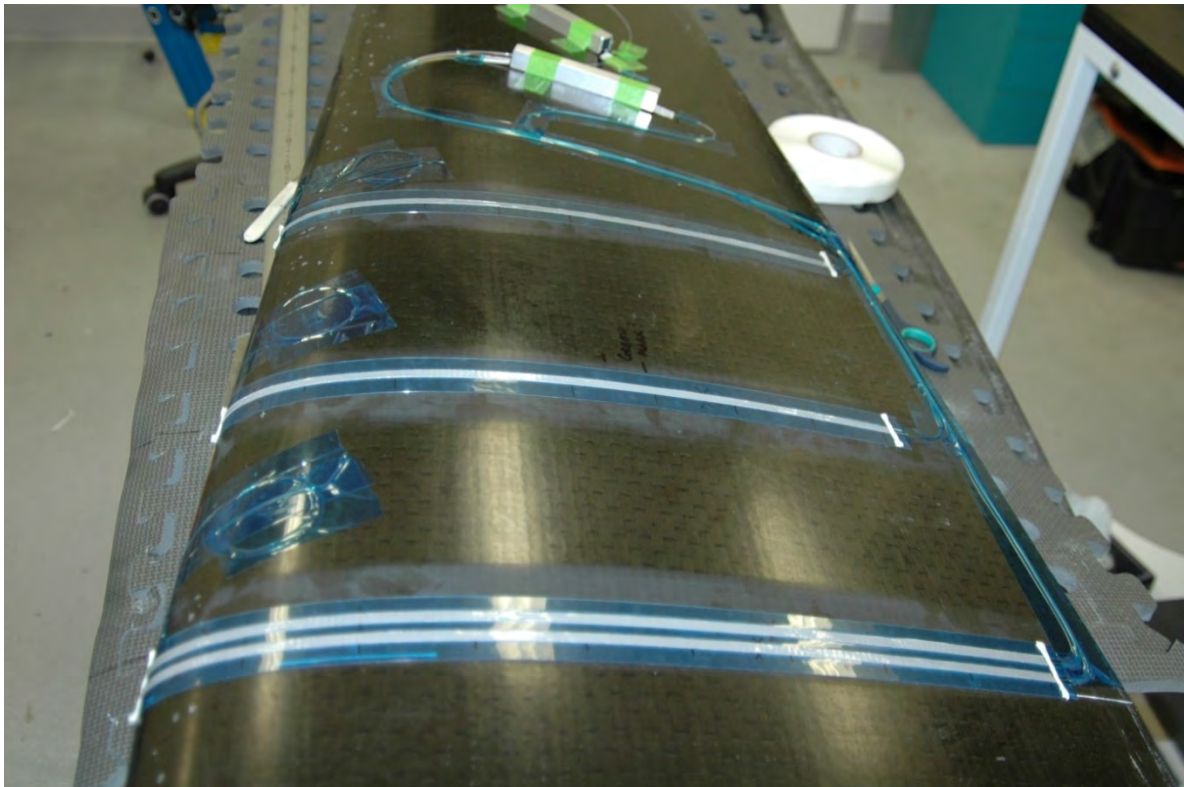
Figure 12: Photo showing the sealing of the chord wise channels using vacuum sealant tape.

The channels were then vacuum bagged on the top and bottom sides of the foil and the part is placed in the oven to cure.

3.4.4 Cure Process

The recommended cure cycle for Redux 312 is 30 minutes at 120 °C which is too high for many epoxy resin based composite systems. However, there are also alternative cure cycles provided by the manufacturer for longer cures at lower temperatures. A previous investigation into the performance of this film adhesive as a methodology for attachment of FBG sensors determined a lower temperature cure cycle (4 hours at 80 °C) which maintained the material strength and performance [10]. This cure cycle was used to attach all the FBG arrays to the hydrofoil.

Figure 13: Hydrofoil in autoclave oven prior to curing.

4. Experimental Setup

The hydrofoil was tested in a custom built load controlled servo-hydraulic fatigue rig. A schematic drawing of the rig is shown in Figure 14. The foil was gripped at its root end by a profiled aluminium capture block. Load was applied near the tip of the foil by a profiled aluminium form board connected to a 280 kN capacity hydraulic actuator. Rubber inserts were used to limit any slippage and ensure the capture block and form board did not appreciably influence the foils structural integrity during the test. Torque on the capture block bolts and form board were checked during the test to ensure no loosening or slippage took place as the test progressed.

4.1 Control System

The control system employed a customised microprocessor based control unit. The unit was designed and built at DST Melbourne and utilized a control algorithm based on a classic load control with an interlock designed to isolate the hydraulic power from the test article in the event of any of the system limits being reached.
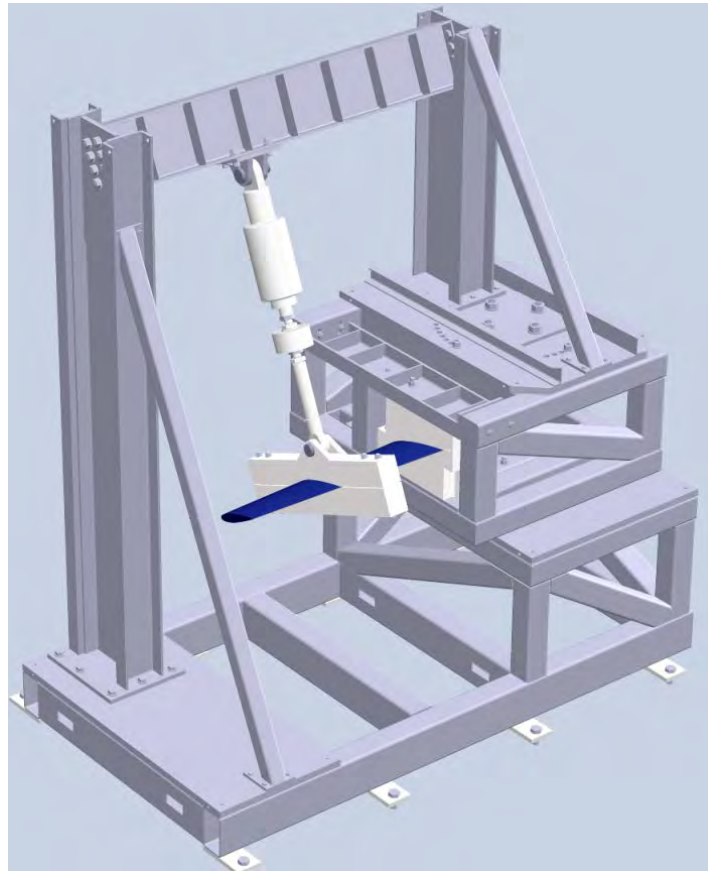
Figure 14: Schematic diagram of servo-hydraulic assembly for application of loads to test hydrofoil.

4.2 Data Acquisition System

An integrated data acquisition system was developed to synchronously record strains measured by the electrical foil strain gauges (FSGs) and optical FBG sensors on the foil. Both the FSG and FBG acquisition systems comprised COTS hardware with custom software developed to enable live visualization of the data and to synchronise the strain data with the load control system.

The FSG acquisition system utilised a National Instruments Ethernet chassis (NI cDAQ-9188XT) incorporating seven quarter-bridge strain modules (NI 9236) to give a total of 56 strain channels. The system also employed a National Instruments (NI 9212) universal analogue input module with 4 general purpose analogue inputs. The cDAQ-9188XT records data to a host PC using via Ethernet connection, the chassis also has two BNC connectors providing digital trigger channels.

DST-Group-TN-1438

The FBG acquisition system consisted of a Micron Optics sm130 optical sensing interrogator combined with a sm041 channel multiplexer which provided 8 channels, each capable of interrogating an array of FBG sensors. The sm130 system also relays data back to a host PC via Ethernet and provides a pair of digital trigger/sync in/out channels.

Both systems asynchronously collect data that is relayed back to a host PC via Ethernet and each acquires data on its own internal system clock. The sm130 provides a hardware synchronisation signal designed to facilitate the synchronisation of data collection between multiple sm130 units. The synchronisation signal consists of a single pulse, which occurs when the interrogator takes a reading, followed by a 32-bit binary-coded decimal integer, which corresponds to the serial number of the data packet that is sent back to the host PC. By modifying the behaviour of one of the digital trigger channels on the cDAQ-9188XT it was possible to record the time of this synchronisation pulse relative to the strain gauge acquisition clock and decode the 32-bit serial number. Using this information it was possible to resynchronise the recorded FBG data relative to the FSG data in post-processing to a high degree of accuracy.

Synchronisation between the Control and FSG systems was achieved with a simple pulse, emitted by the control system at the start of each measurement block, which was recorded using the second digital trigger channel on the cDAQ. In order to compensate for clock-drift between the acquisition systems over long measurement blocks, a secondary synchronisation method was also included. This involved splitting the signal returned by the load-cell such that it could be simultaneously recorded by both the control system and the cDAQ using one of the analogue inputs on the NI 9212 module. This shared analogue load signal could be used to resynchronise the data using cross-correlation if necessary.

The customised control software for the FBG system was developed using a mix of C++ for low-level decoding and processing of the raw data stream from the sm130 and Python for high-level control tasks and the user interface. Given the high sensor-count afforded by the FBG acquisition system it is possible to display a 2D strain-map visualisation in "real-time" while the structure is under load. The user-interface and strain visualisation was developed using the open-source PyQtGraph library to provide a "real-time" interpolated strain-map from the array of strain data and a scrolling time-history of strain data for a selectable subset of sensors. The software was capable of recording all of the measured FBG wavelengths, FBG peak-detection status information, and the packet serial numbers. In addition, all of the configuration settings, including sensor x-y coordinates, 'zero' wavelengths and strain map settings are stored in each data file, allowing the strain-map to be easily re-created offline.

The software for the FSG system was developed using LabVIEW. It was designed to record and display incoming strain data from the cDAQ, while also decoding and storing the synchronisation information from the FBG and control systems. Strain visualisation was provided by a scrolling time-history plot of one or more strain channels. A simple 'alarm' system was also included to indicate potential failure of strain gauges that had moved beyond a pre-defined range.

The data format chosen for both the FSG and FBG acquisition systems was HDF5, an open-source binary file format designed for storing large quantities of numerical data. It was chosen in preference to a plain text format such as CSV because it offers far more compact storage along with significantly faster random access to data, while still being an open and well supported format.

As the data acquisition is shared between three different systems, time-synchronisation of all the channels must be performed in post-processing. The data acquisition systems and control system were all set to record data at similar rates. The Control system recorded at ~39 Hz, the FBG system at 50 Hz and the FSG system at 40 Hz. A post-processing script was created to synchronise the FBG and control system channels with the FSG system channels by interpolating the FBG and control channels onto the FSG system clock. The post-processing script creates a synchronised dataset combining all load, displacement, FBG and FSG strain sensors.

4.3 Test Schedule

A series of dynamic loading profiles which increased in amplitude were applied to the test foil as outlined in Table 1. At the start and completion of each cyclic load level static load surveys were conducted. For the static loading tests, load increments were applied in 1.4 kN steps followed by an 8 second dwell time to allow for sufficient averaging of data at that load step. The load was incrementally increased in this way up to the maximum load where it was then held for 60 seconds. After this dwell the load was incrementally reduced in the same way back to zero load. Each static load profile was typically repeated three times to allow for the run-to-run reproducibility to be assessed.

One of the primary objectives of the test was to generate a fatigue failure. Accordingly, the fatigue loads were progressively increased until failure occurred in the time available for testing. A sinusoidal cyclic load profile was applied for the fatigue loading tests. The fatigue stress range was always single direction i.e. not full reversal. The ratio of minimum to maximum stress for each cycle (R-ratio) was less than 0.25, which represents a relatively severe stress range condition.

Table 1: Summary of key parameters from the structural fatigue test.

Peak Load (kN)	Peak wire strain SG # 2 (μe)	Peak LE Tip Deflection (mm)	Cycles
28	1940	39.5	74 266
35	2460	51.5	39 500
49	3090	62.5	57 000
62	4140	85.5	25 500

5. Results

5.1 FBG Spectral Response

As outlined in the background section of this report, uniform changes in strain along the axis of an FBG sensor will result in a shift in the peak wavelength of the reflection spectrum. A compressive strain will result in a reduction in peak wavelength and a tensile strain will result in an increase in peak wavelength. If changes in the spectral reflection shape occur this implies a non-uniform strain along the sensor length. Changes in spectral shape also make it difficult to employ standard FBG interrogation schemes to measure strain changes as these interrogation schemes typically rely on simple peak tracking algorithms. Figures 15 to 18 show the reflection spectra from the four span wise (see Figure 5) FBG arrays after attachment to the test article by thermal cure. The FBG sensors on all arrays show a narrow band peak reflection indicating that the attachment process did not induce a strain gradient across the sensors.
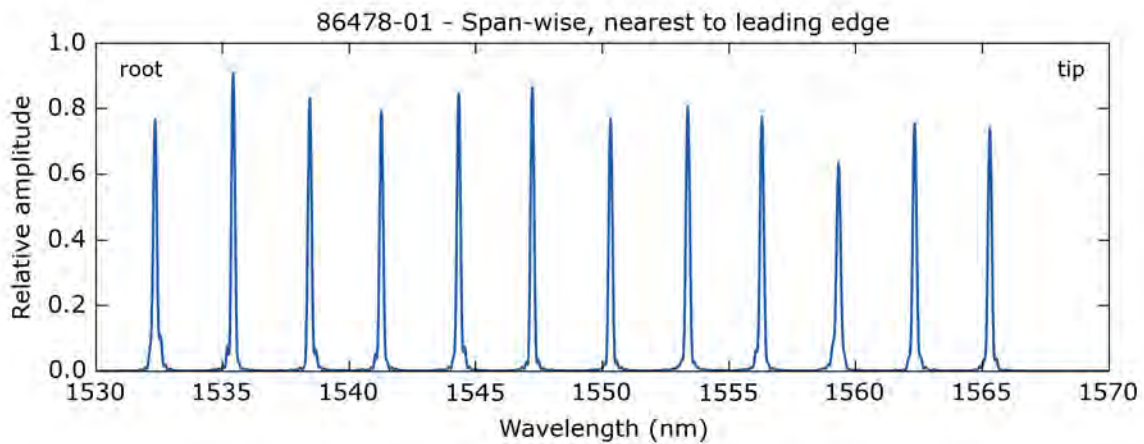
Figure 15: Reflection spectra from the span wise FBG array nearest to the leading edge after attachment to part.
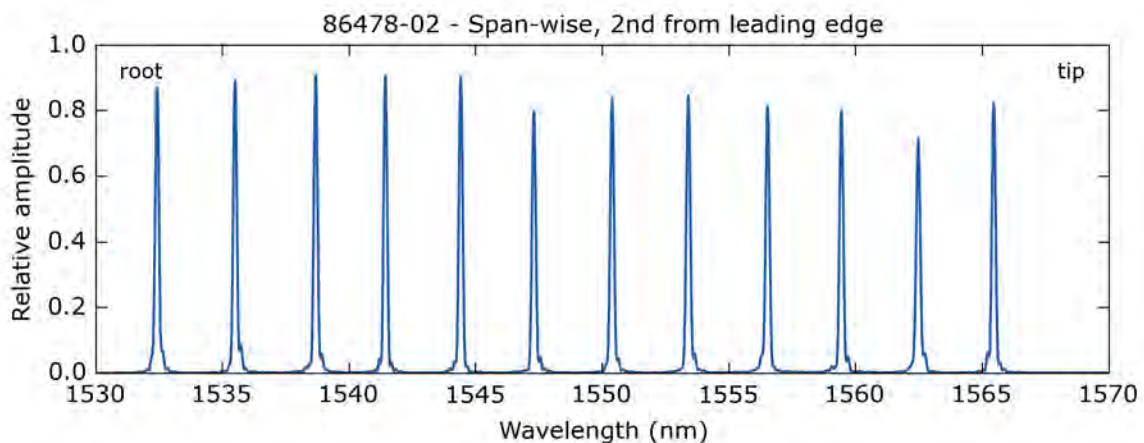
Figure 16: Reflection spectra from span wise FBG array 2nd from the leading edge after attachment to part.
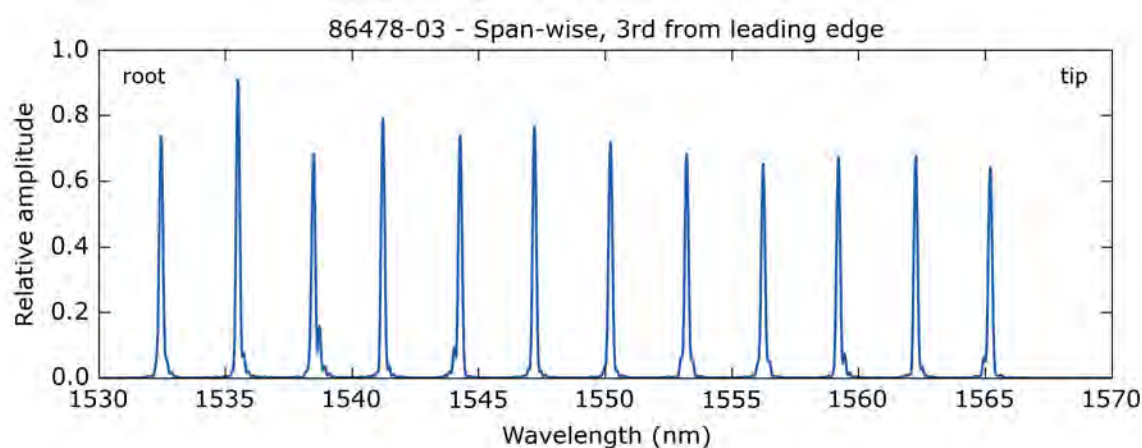
Figure 17: Reflection spectra from span wise FBG array 3rd from the leading edge after attachment to part.
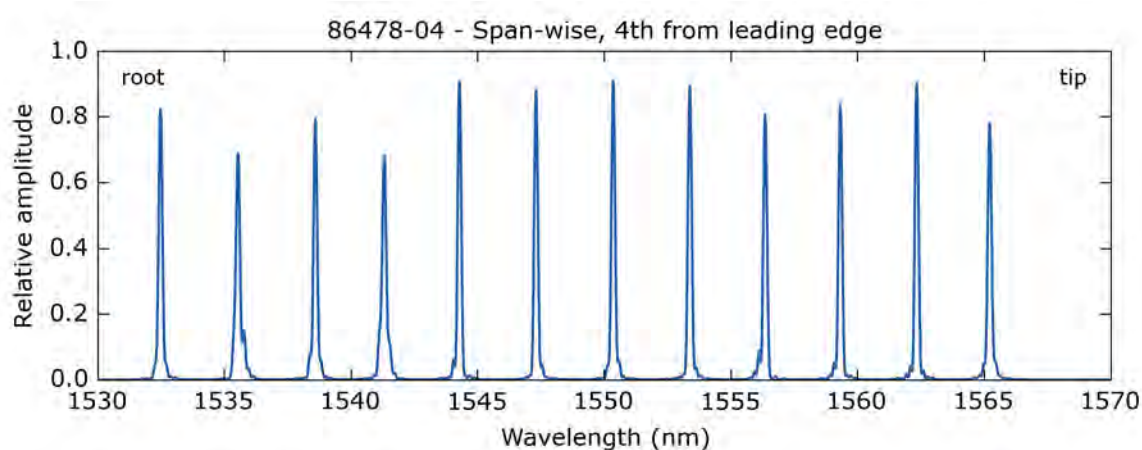

Figure 18: Reflection spectra from span wise FBG array 4th from the leading edge after attachment to part.

Figures 19 to 22 show the reflection spectra from the four chord wise (see Figure 6) FBG arrays after attachment to the test article. In this orientation there is evidence of significant changes to reflection spectral profiles of the FBGs particularly near the leading edge of the blade. The FBG reflection spectra all had narrow band profiles before attachment so this implies that the attachment process has induced a strain gradient along the FBG gauge length. There are two proposed hypotheses for the cause of this gradient. One is that the curvature of the blade (which is more significant in the chord wise orientation, particularly near the leading edge) has induced a strain gradient in the fibre during the lay-up process. The second hypothesis is that the variation in thickness of the part results in a thermal gradient during the cure process which sets in a strain gradient during the cooling of the resin.

In order to prove which hypothesis is correct it is necessary to monitor the reflection spectrum during the application and cure process on a representative part. Figure 23 shows the reflection spectra from an FBG array attached to a composite propeller blade with a curved geometry similar in profile to the hydro foil. This graph shows a large shift

to the right during the cure process which is caused by the increase in temperature but no change in spectra shape. As the cure cycle finishes a strain gradient is induced in the FBGs during the cooling of the adhesive resin matrix supporting the second hypothesis. This result is significant as it precludes the use of thermal cure processes for attachment of optical fibres on parts with a significant variation in thickness profile.
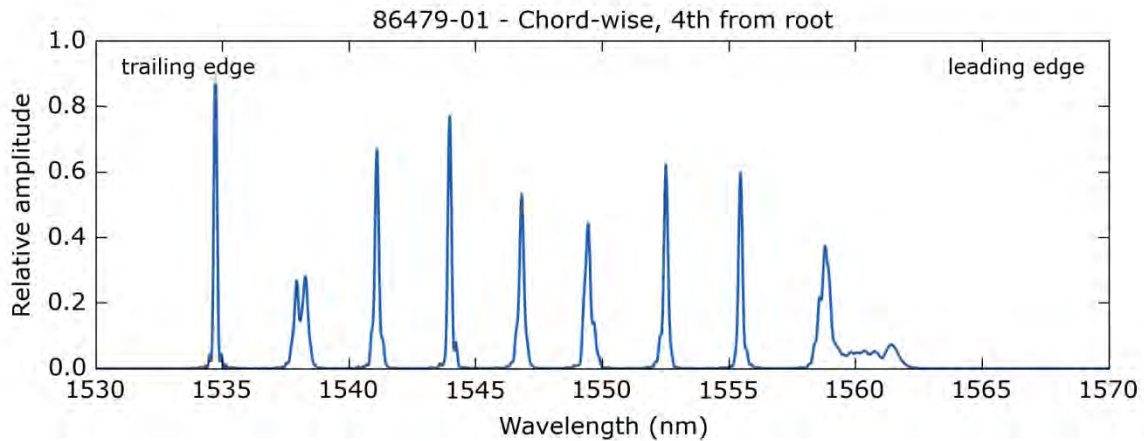

Figure 19: Reflection spectra from the 4th chord wise FBG array from the root after attachment to part.
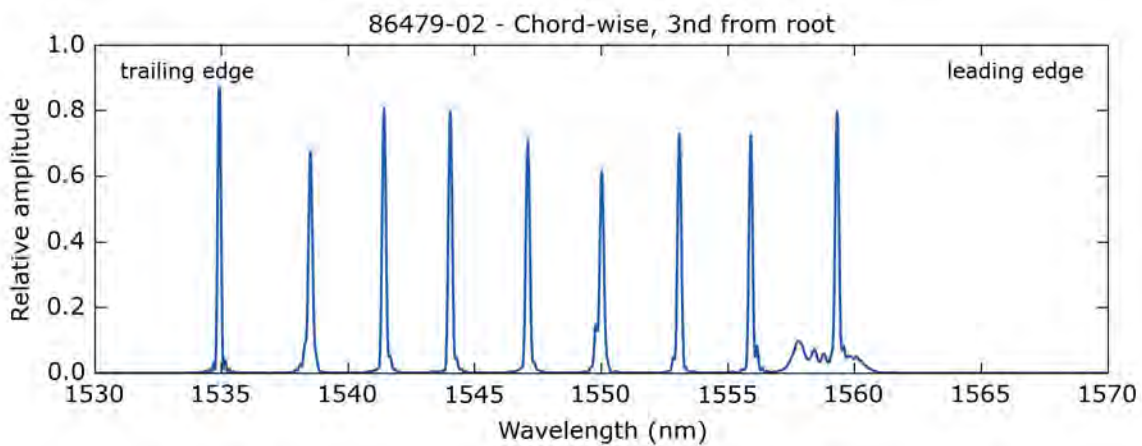
Figure 20: Reflection spectra from the 3rd chord wise FBG array from the root after attachment to part.
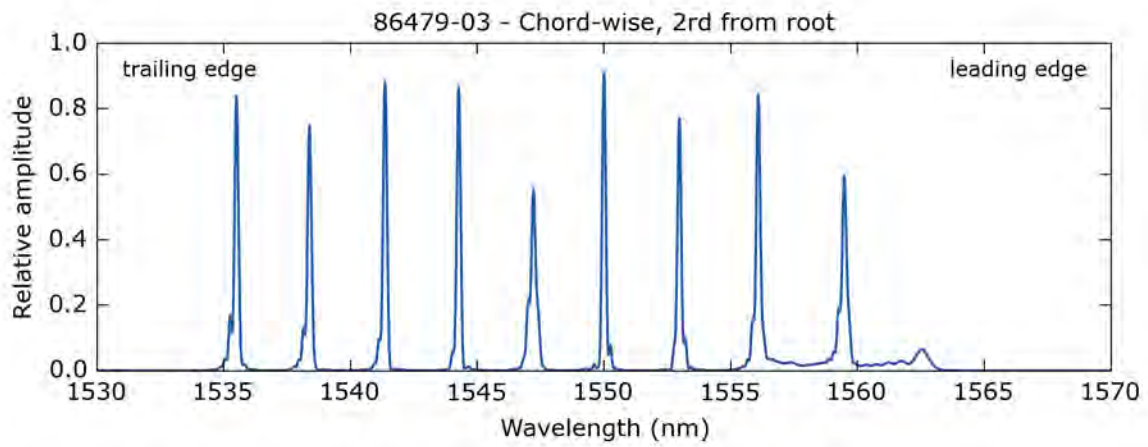
Figure 21: Reflection spectra from the 2nd chord wise FBG array from the root after attachment to part.
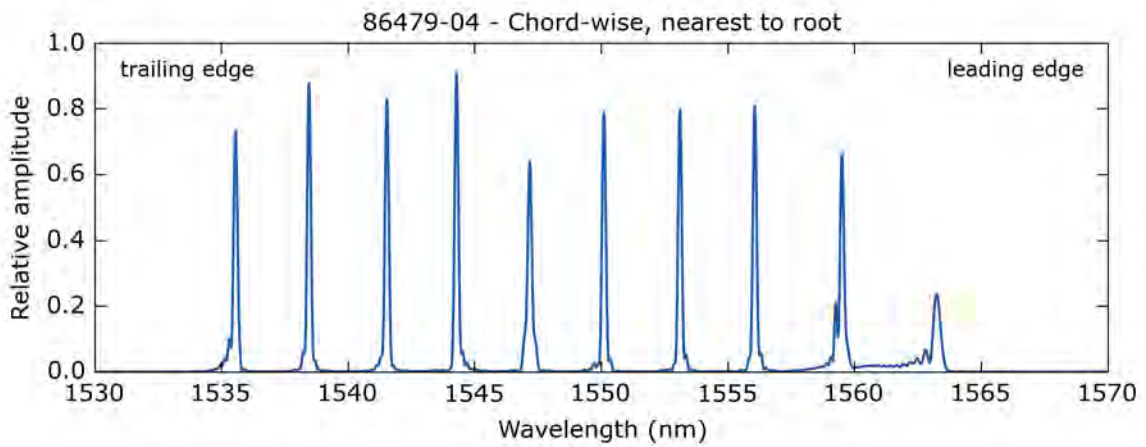

Figure 22: Reflection spectra from chord wise FBG array nearest to the root after attachment to part.
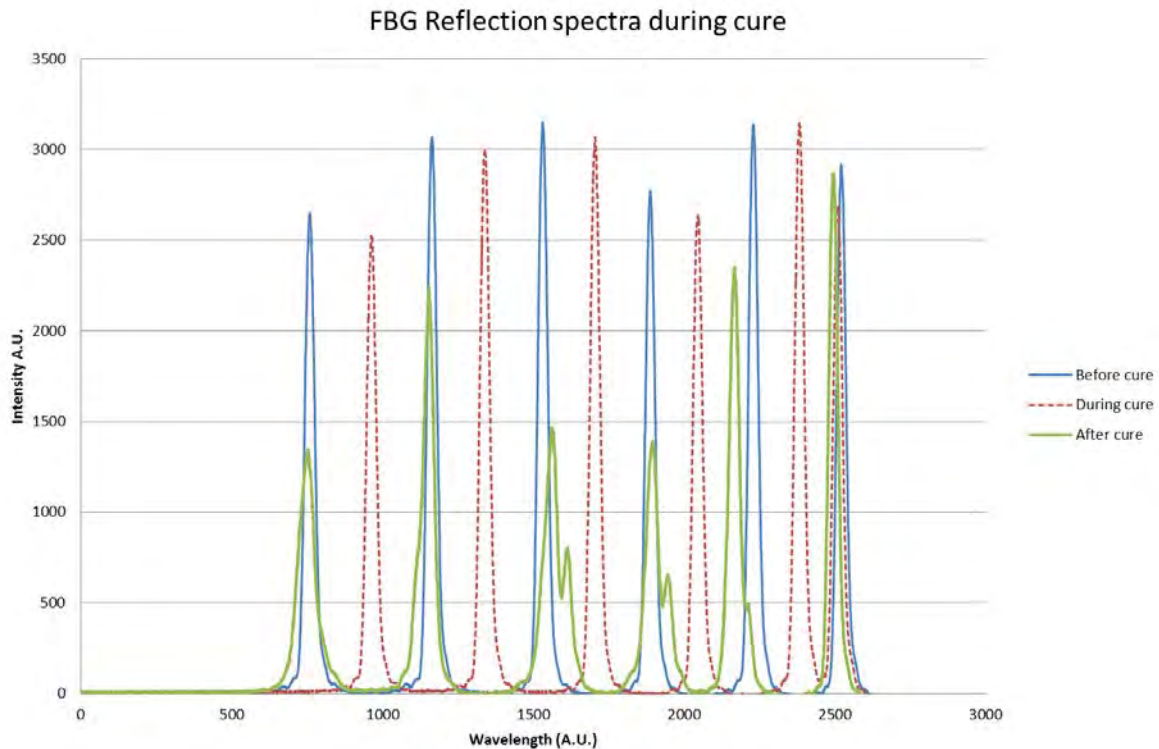
Figure 23: FBG reflection spectra before, during and after the thermal cure process on a composite propeller part with a complex geometry.

The Micron Optics sm130 system which uses a peak tracking algorithm to measure strain from the FBG spectra was unable to measure reliably from the corrupted reflection profiles observed on the chord wise sensors, therefore for most results in the proceeding sections only data from the span wise sensors is presented.

5.2 Static Load Survey

Figures 24 to 27 show the strain response to a static load survey and the hysteresis in response to a 28 kN load from a number of electrical and optical gauge pairs which were located in close proximity to one another on the foil as indicated in Figure 5. The data shows good agreement. Figures 28 to 31 show the linearity of response for the same gauge pairs.

In regions where there is a large gradient and the optical and electrical gauges are not placed closely together or aligned in the same orientation the agreement between the two measurement sets is not as good, as shown in Figure 32. Table 2 summarises the relative difference of the FBG strain measurement relative to the electrical gauge measurement for all of the sensors pairs which were reasonably closely located. The largest differences were observed in the root area where there is a steep gradient near the blade constraining point.

Table 2: Summary of percentage strain differences for optical strain gauges relative to electrical strain gauges (sensor pairs in close proximity).

FBG	Foil gauge	% difference (FBG relative to Foil)
1.1.1	6	-10.00%
2.1.1	10	1.50%
2.1.3	17	-2.50%
2.1.5	21	2.00%
2.1.7	26	-2.00%
2.1.11	28A	4.30%
3.1.1	12	-2.50%
3.1.5	22	3.00%
4.1.1	13	12.00%
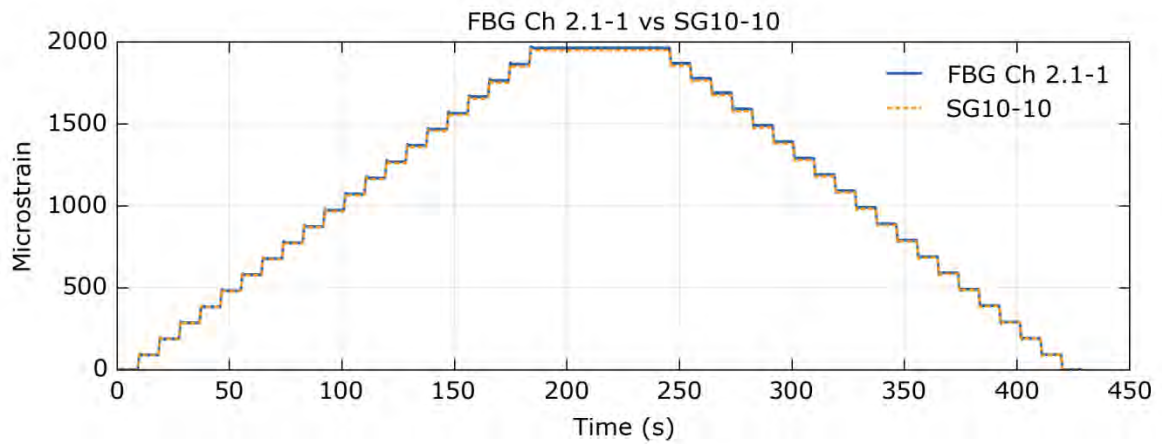
Figure 24: Strain response to static load survey to 28 kN for co-located optical and electrical gauges.
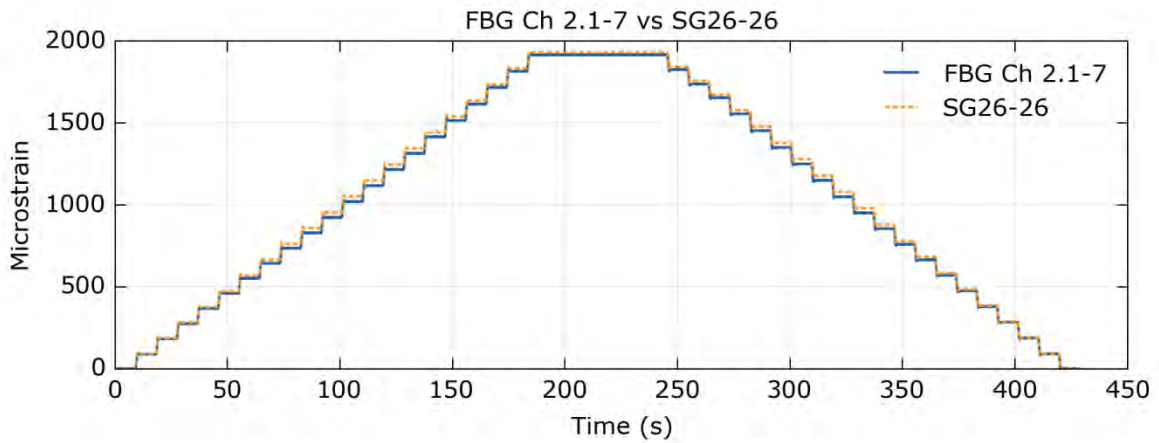
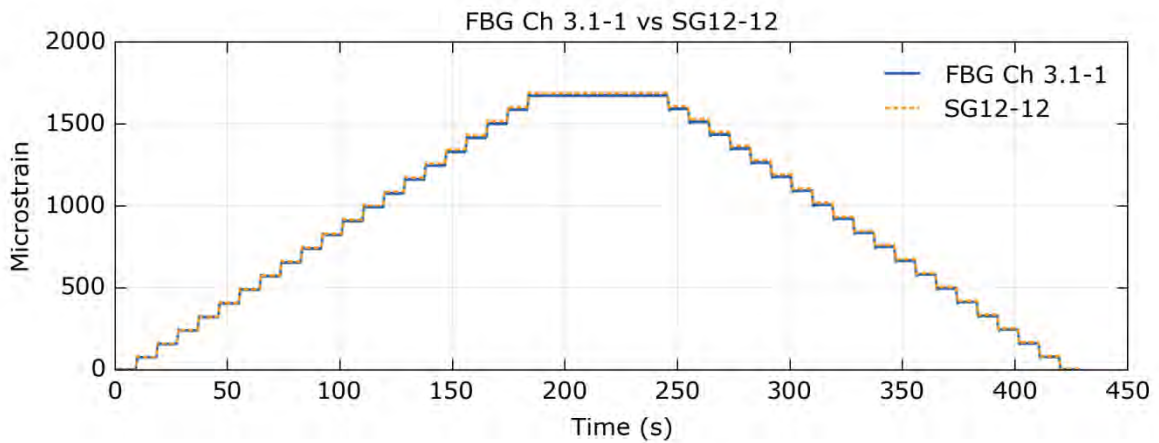*Figure 25: Strain response to static load survey to 28 kN for co-located optical and electrical gauges.*

Figure 26: Strain response to static load survey to 28 kN for co-located optical and electrical gauges.
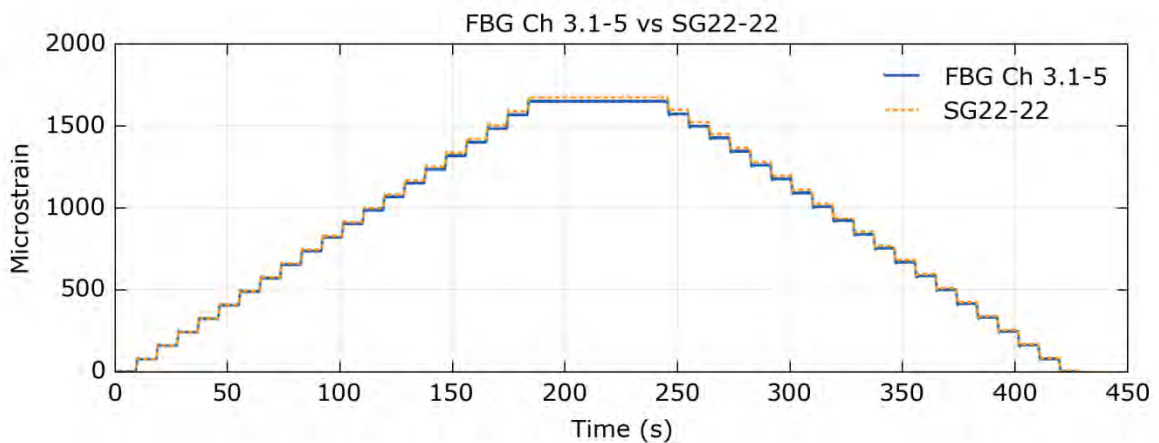

Figure 27: Strain response to static load survey to 28 kN for co-located optical and electrical gauges.
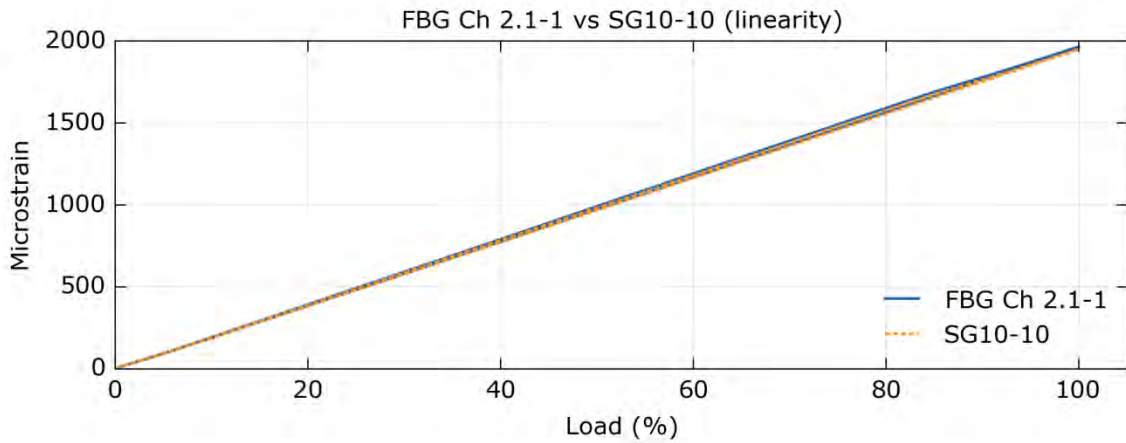
Figure 28: Comparison of linearity of strain response to 28 kN for co-located optical and electrical gauges.
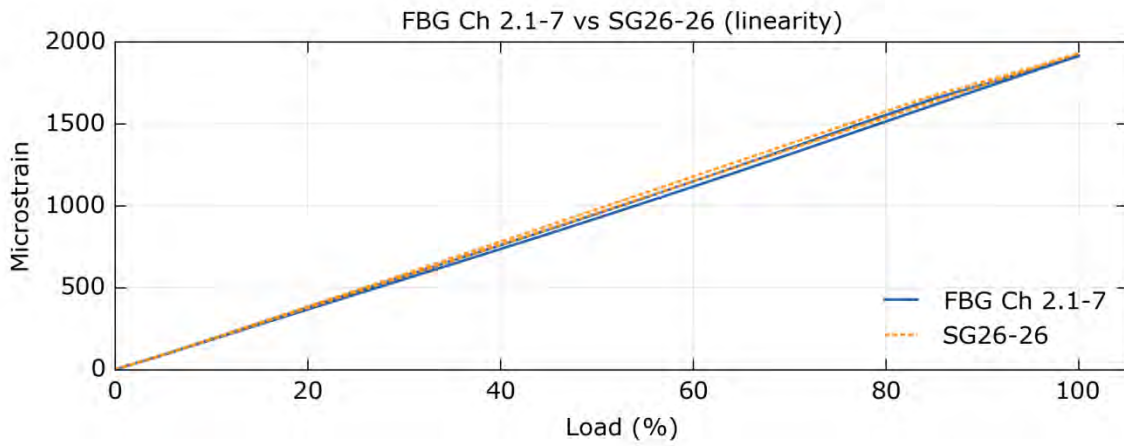

Figure 29: Comparison of linearity of strain response to 28 kN for co-located optical and electrical gauges.
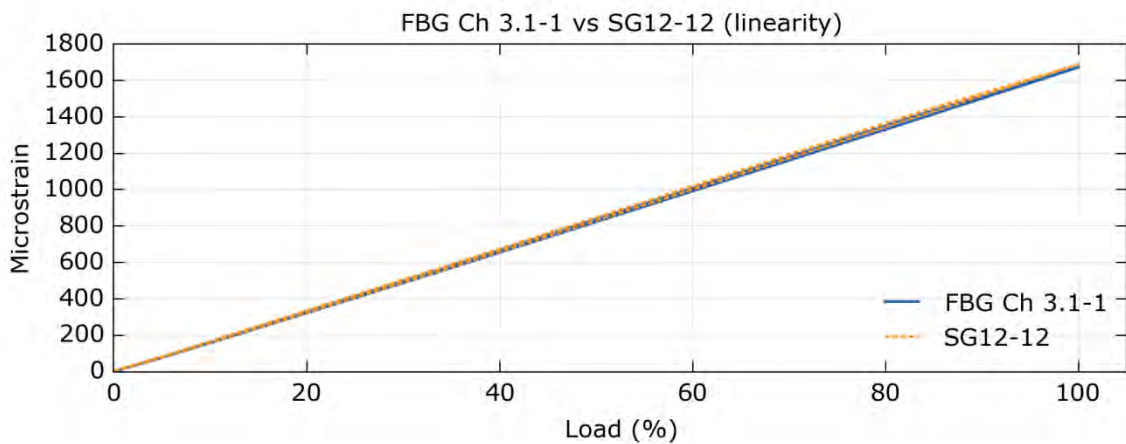

Figure 30: Comparison of linearity of strain response to 28 kN for co-located optical and electrical gauges.
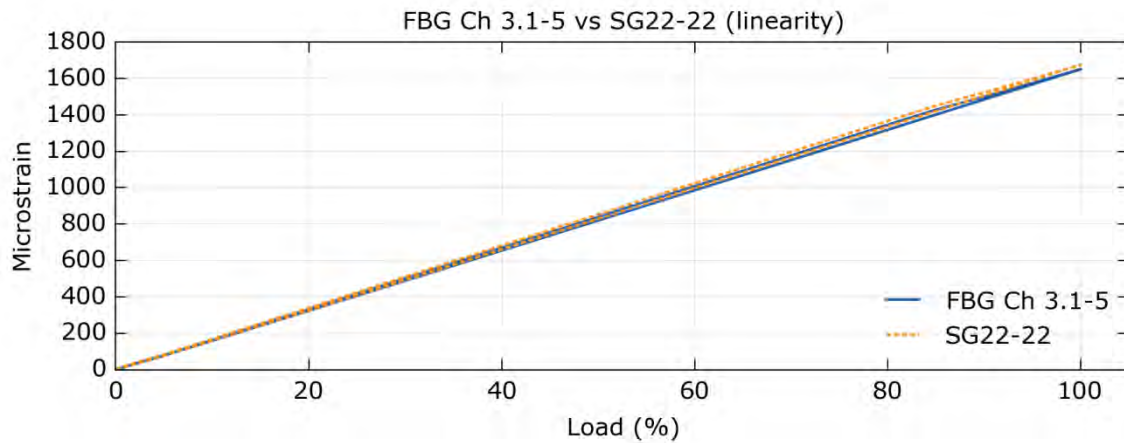
Figure 31: Comparison of linearity of strain response to 28 kN for co-located optical and electrical gauges.
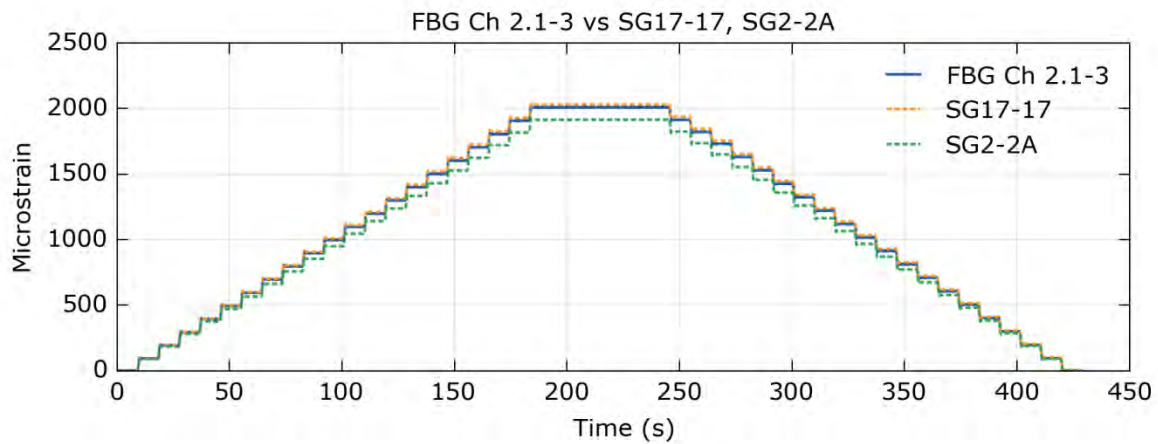

Figure 32: Strain response to static load survey to 28 kN for co-located optical and electrical gauges (SG2-2A slightly offset from FBG sensing location).

Because of the high number (48) of FBG strain measurements it is also possible to generate a relatively coarse strain map in the span wise direction from experimental data and compare this to the strain map generated from an initial FEA model of the hydrofoil as shown in Figure 33. The experimental and modelled distributions for an applied load of 28 kN are similar in distribution and amplitude. However, further refinements to the model are required to enable a detailed numerical point by point comparison. The refinements that are to be made include: measuring the properties of the constituent materials by coupon tests, determination of the achieved fibre volume fraction and determination of the achieved ply thickness.
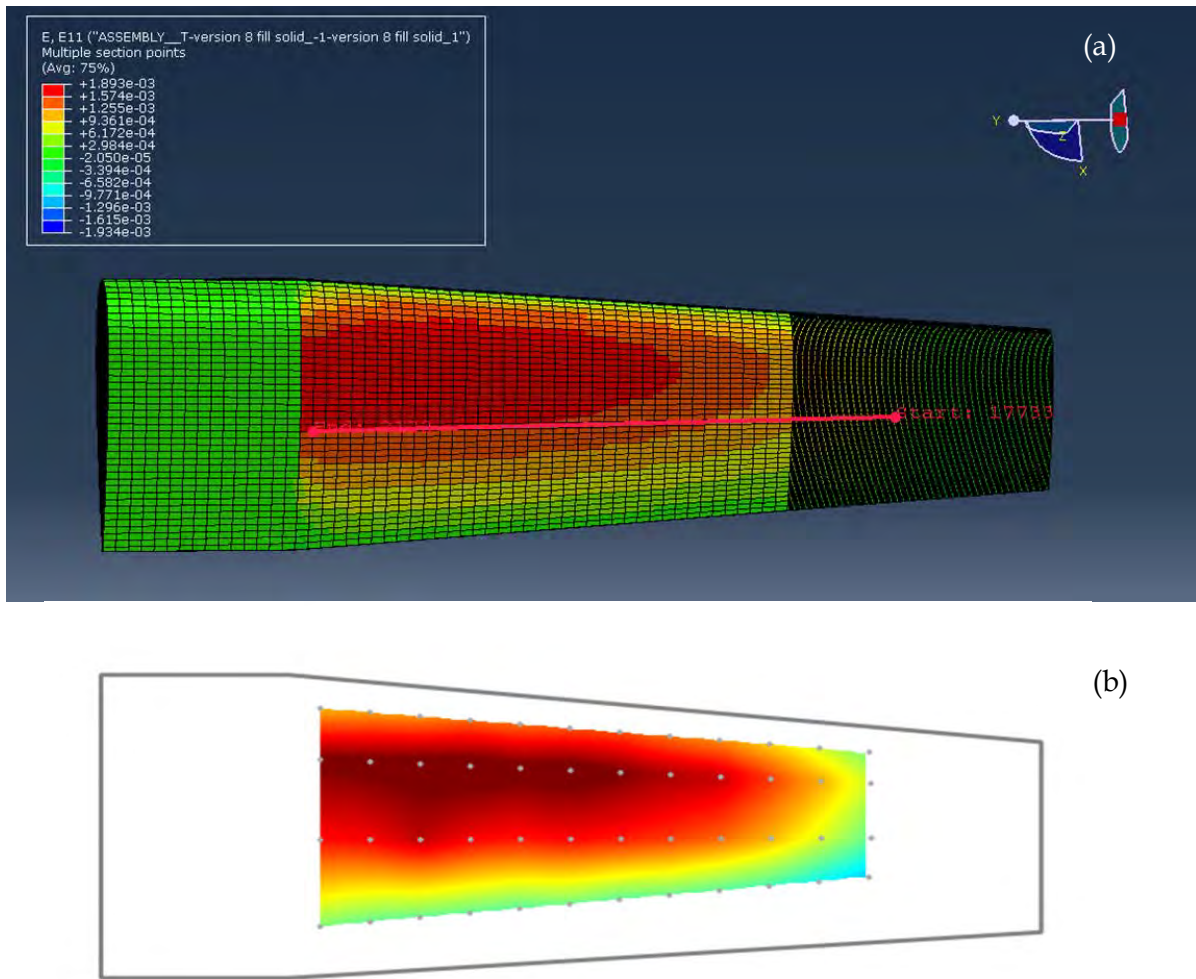
Figure 33(a) Strain map of the foil upper side as predicted by FEA for a load of 28 kN; (b)Strain map of the foil upper side using experimental strain data from FBG sensing arrays for a load of 28 kN.

5.3 Foil Failure

The hydrofoil failed under fatigue loading during its last phase of cycling after 25,500 cycles under a peak load of 62 kN. Under this load large deflections and peak strains were seen in the order of 75 mm and 4000 µε, respectively. Upon physical inspection, failure occurred on the bottom half of the foil near the root region at the interface of the carbon structural plies and the glass core plies. Visible damage along the span of the hydrofoil was minimal with some delamination near the bondline on the leading edge near the root and crazing along the leading edge up to mid span length. A CNC waterjet cutter (TECHNI model TJ3000-x2) was used to cut a transverse section out of the root end of the foil. The section was polished and then photographed. The crack spans from the leading edge to the trailing edge. Near the leading edge of the foil, in the structural carbon plies, the crack is jagged and lies just below the bondline as shown in

Figure 34(a). Further along the cross section, the crack aligns to where the Glass-Mat layer meets the Glass-Quad core and has remained clearly in this path till the trailing edge as shown in Figure 34(b).
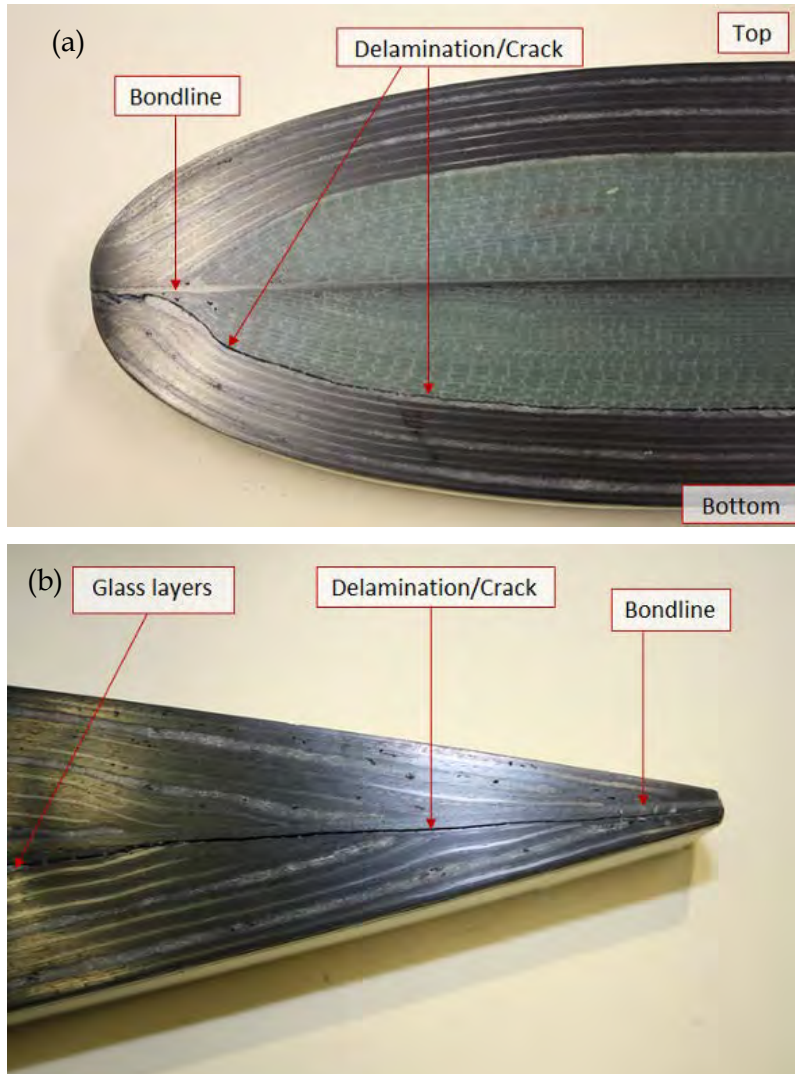

Figure 34: (a) Photograph of root end of foil showing the damage located between the carbon skin and the glass core and (b) Delamination at the Glass-Mat layer/ Glass-Quad core interface.

Figures 35 and 36 show the responses of a co-located FBG and FSG in the highest strain region of the hydro foil post fatigue failure under a static strain survey to 49 kN. Both sets of gauges continue to compare well in terms of the strain values but show a significant increase in hysteresis after failure as a result of the compliance changes induced in the foil. This hysteresis was typical of that observed from all of the gauges across the part.
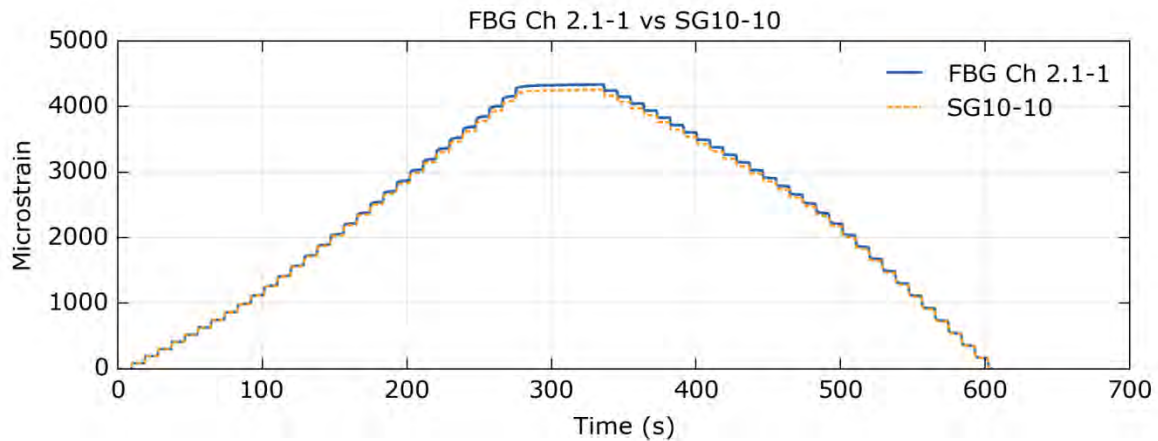
Figure 35: Strain response to static load survey to 49 kN for co-located optical and electrical gauges post failure of the hydro foil.
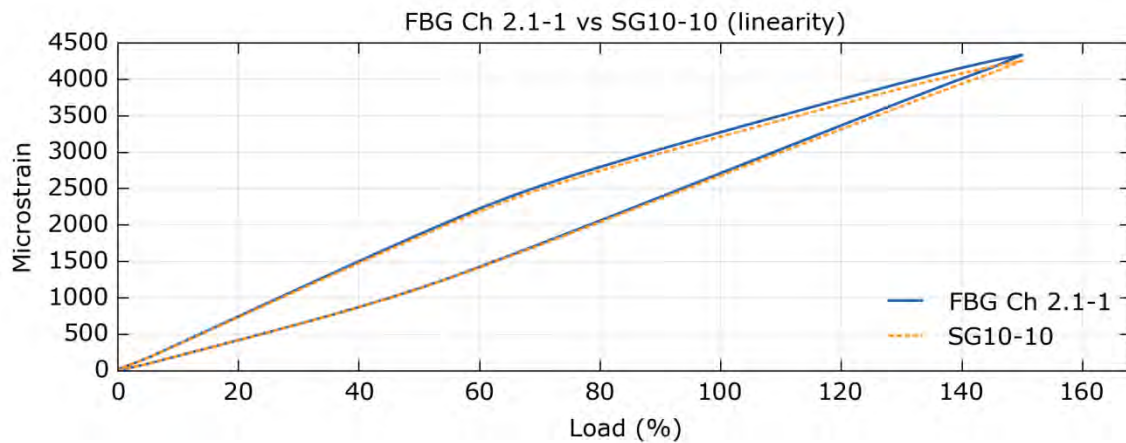

Figure 36: Comparison of linearity of strain response during loading and unloading to 49 kN for co-located optical and electrical gauges post failure of the hydro foil.

Figure 37 to 40 show the unloaded reflection spectra from each of the span wise arrays before and after failure of the part. There is a slight increase in strain in the centre of the foil near the root after failure of the part in the span wise direction. The reflection spectra from the FBG arrays in the chord wise direction were also examined pre and post failure as shown in Figures 41 to 44. In this case there was a significant increase in strain for the gauges nearest to the leading edge in the region where the primary failure occurred. For the case of the array closest to the root, there is an increase in strain of approximately 3500 μstrain in the region where the top and bottom halves of the foil debonded. There is also evidence of a strain gradient at even higher levels in this region.
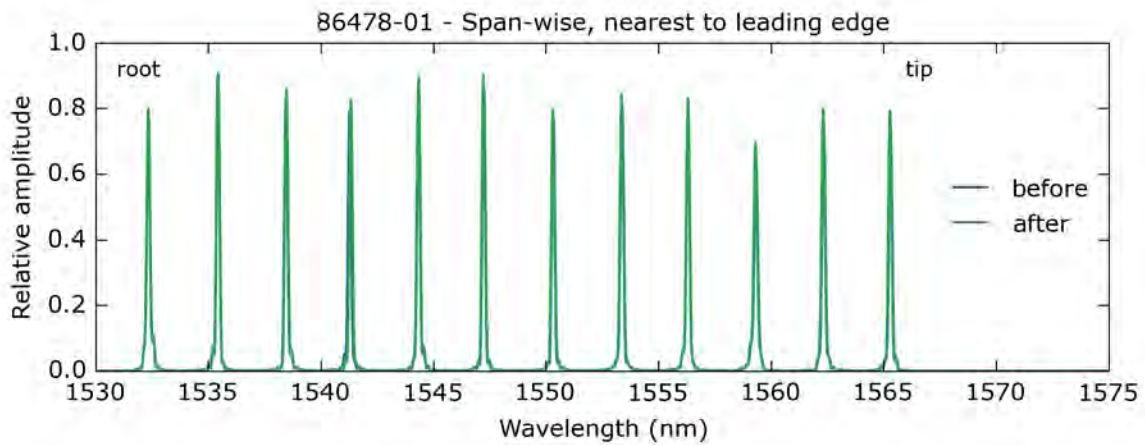
Figure 37: Reflection spectra before and after foil failure from span wise FBG array nearest to leading edge.
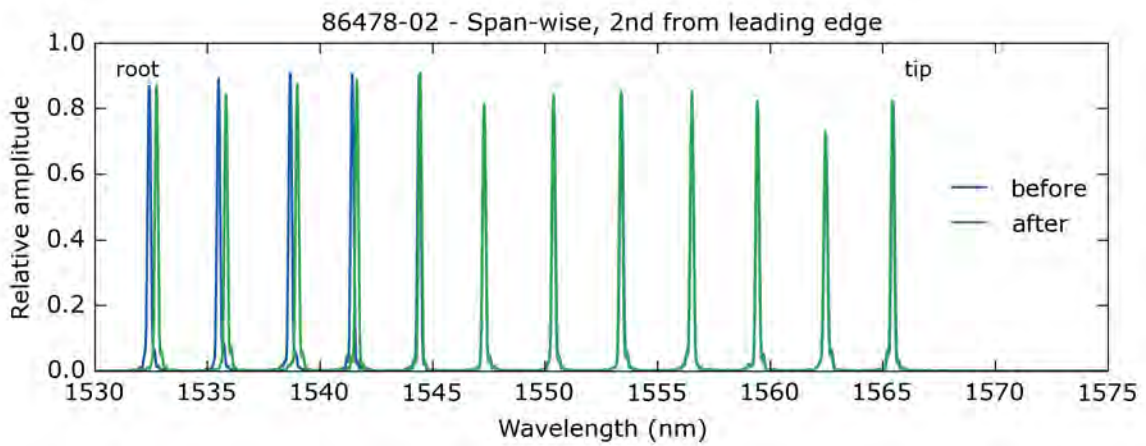

Figure 38: Reflection spectra before and after foil failure from span wise FBG array second from leading edge.

Figure 39: Reflection spectra before and after foil failure from span wise FBG array third from leading edge.

Figure 40: Reflection spectra before and after foil failure from span wise FBG array closest to trailing edge.

Figure 41: Reflection spectra before and after foil failure from chord wise FBG array closest to trailing edge.
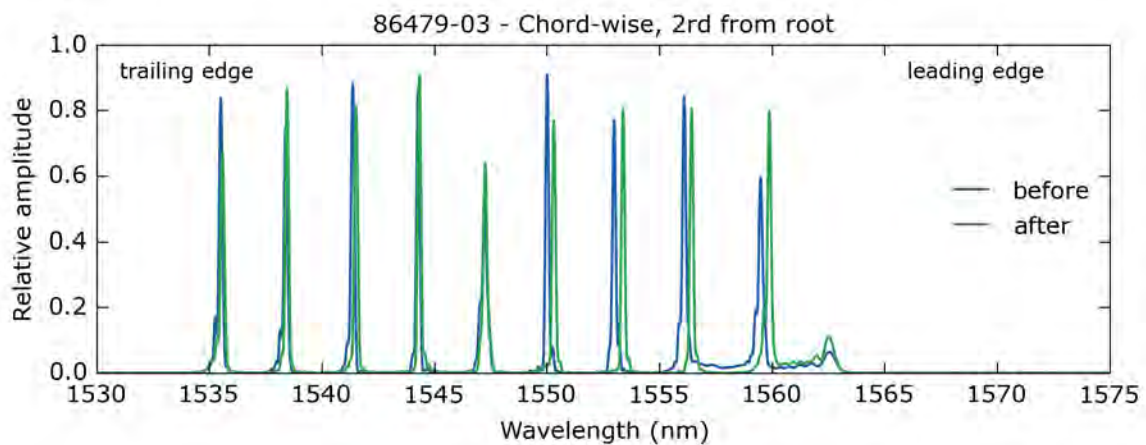
Figure 42: Reflection spectra before and after foil failure from chord wise FBG array second closest to root.
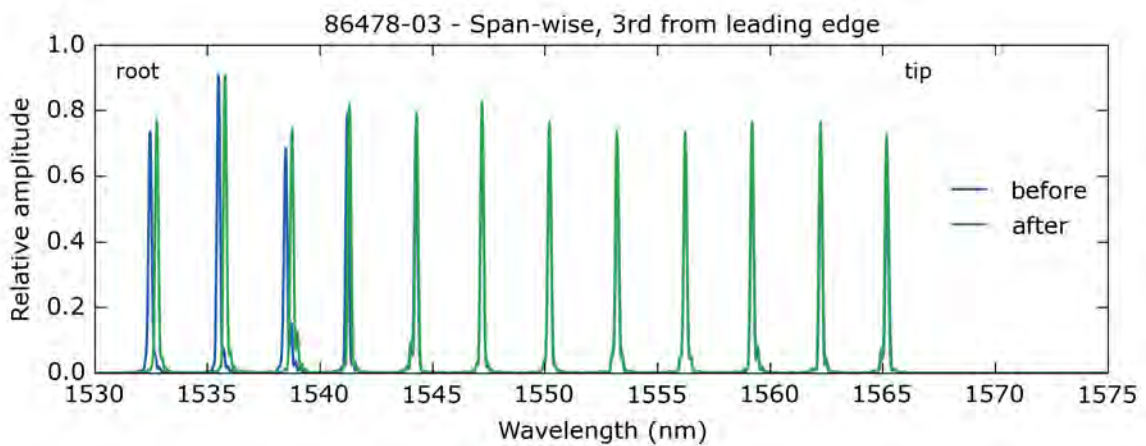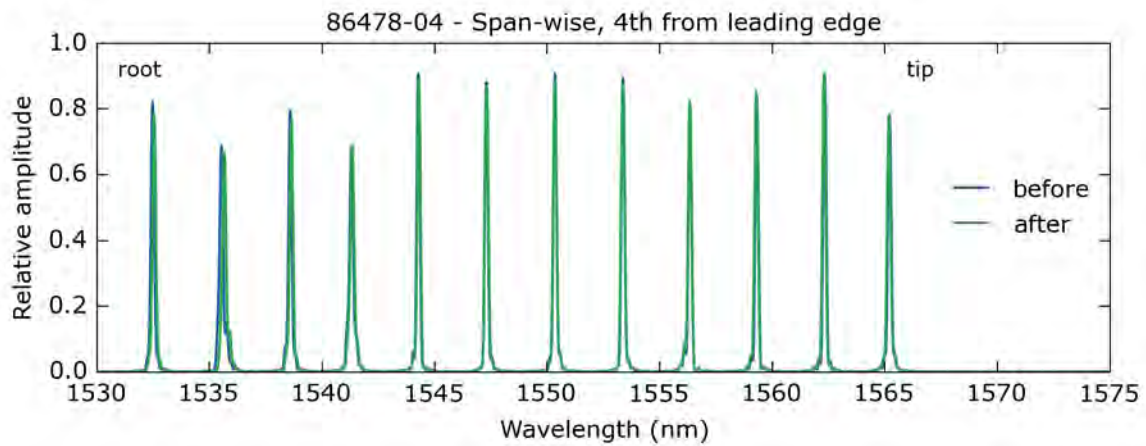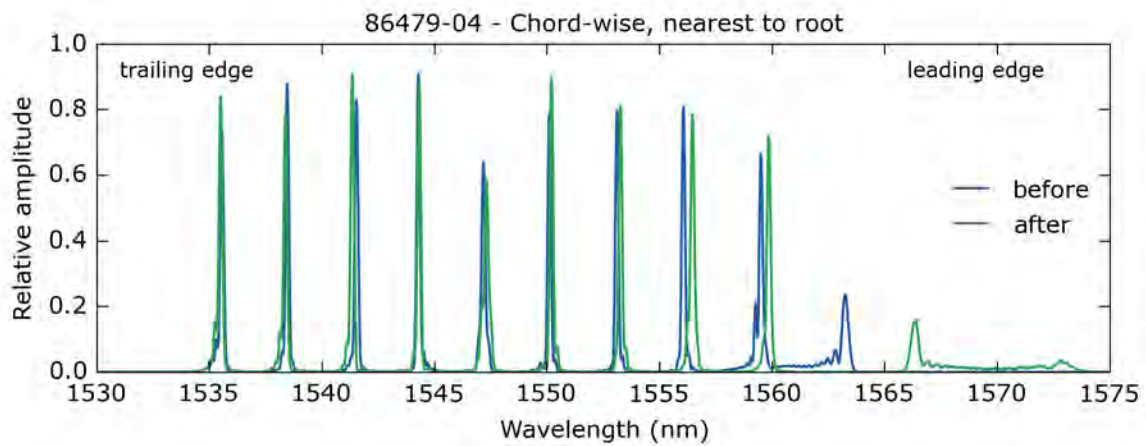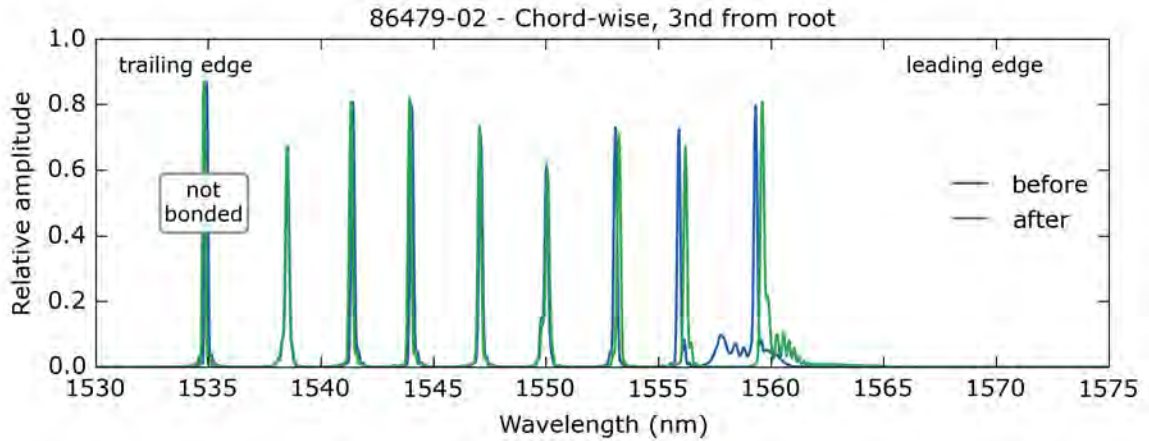
Figure 43: Reflection spectra before and after foil failure from chord wise FBG array third closest to root.
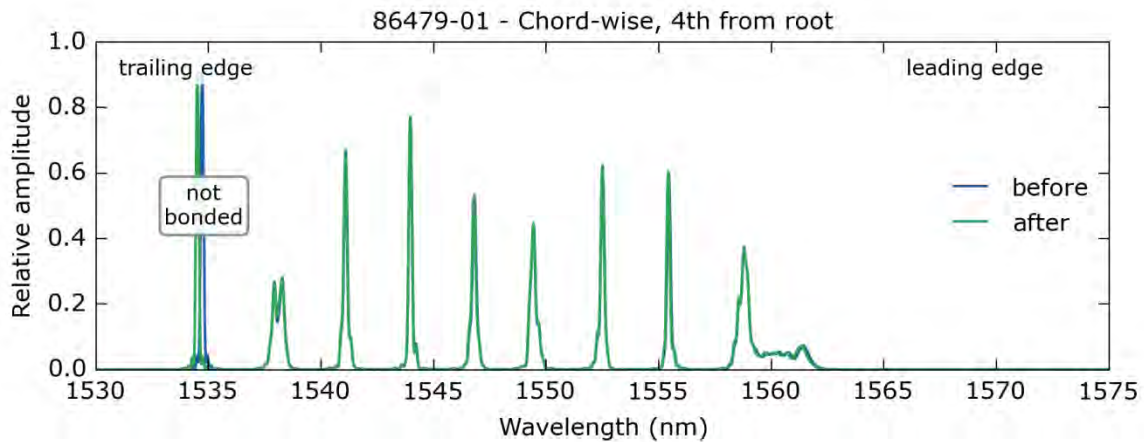
Figure 44: Reflection spectra before and after foil failure from chord wise FBG array fourth closest to root.

6. Analysis and Conclusions

The results presented confirm that FBG arrays may be surface-mounted with minimal intrusion to a large composite structure and used to provide detailed strain distribution information from across the surface. The measured strain values from the FBG sensors agreed well with data from co-located electrical strain gauges and with model predictions. Both the optical and electrical strain data detected a large change in compliance after critical failure of the part.

The attachment methodology using Redux 312 film adhesive was durable and the sensors and their packaging survived fatigue loading until failure of the part and beyond. The impact on the surface profile of the part was minimal with a raised profile of approximately 400-500 microns in the bonded region.

However a significant result to emerge from this testing was the discovery that the thermal cure process introduced a strain gradient in the sensor in regions where there was a significant thickness variation in the part in the direction of the sensing fibre. This strain gradient was induced during the cooling of the adhesive and attributed to the irregular thermal profile induced by the thickness variation. The strain gradient results in an irregular reflection spectrum from the FBGs which makes it difficult to interrogate the gratings using the standard peak tracking algorithms which are employed by most commercial-off-the-shelf (COTS) systems.

For the hydrofoil experiment the implications of this gradient meant that it was not possible to reliably make measurements in the chord wise direction where the change in thickness was most pronounced. More broadly the significance of this result is that this attachment methodology is not suitable for the measurement of surface strains on the composite propeller planned for the AMP trial which has a complex geometry and a substantial variation in thickness across the part.

Having said that, the concept of using high density FBG arrays to map surface strains has been demonstrated and validated and should be feasible on a composite propeller with the use of an appropriate room temperature cure adhesive. Further testing will be required to validate this adhesive for in the service environment.

7. References

[1] Overview of Lead-in Activities for the Advanced Material Propeller Structural Fatigue Test Program. Andrew Phillips, Asintha Nanayakkara, Russell Cairns, Nigel St John, Robert Ditchburn, Matthew Ibrahim, Claire Davis, Patrick Norman and Peter Smith. (2015) *DST Technical Report*, (in preparation).

[2] Fiber Bragg grating technology fundamentals and overview. Hill, K.O., Meltz, G.(1997) *Journal of Lightwave Technology*, 15 (8), pp. 1263-1276.

[3] Fiber grating sensors. Kersey, A.D., Davis, M.A., Patrick, H.J., LeBlanc, M., Koo, K.P., Askins, C.G., Putnam, M.A., Friebele, E.J. (1997) *Journal of Lightwave Technology*, 15 (8), pp. 1442-1462.

[4] High mechanical strength single-pulse draw tower gratings, M. Rothhardt, C. Chojetzki, and H. R. Mueller *Proc. SPIE(North 2004: Photonic Applications in Telecommunications, Sensors,Software, and Lasers)*, vol. 5579, pp.127–135.

DST-Group-TN-1438

[5] Surface Preparation for Strain gage Bonding. Micro measurements Instruction Bulletin B-129-8. Revision 08-07-14. http://www.vishaypg.com/docs/11129/11129B129.pdf

[6] Strain Gage Installations with M-Bond 200 Adhesive. Micro measurements Instruction Bulletin B-127-14. Revision 10-14-11.
http://www.intertechnology.com/Vishay/pdfs/Instruction_Bulletins/B-127-14.pdf

[7] Strain Gage Applications with M-Bond AE-10, AE-15, and GA-2 Adhesive Systems. Micro measurements Instruction Bulletin B-137-4. Revision 07-16-14.
http://www.vishaypg.com/docs/11137/B137-4-.pdf

[8] High-Strain Fiber Bragg Gratings for Structural Fatigue Testing of Military Aircraft. Claire Davis, Silvia Tejedor, Ivan Grabovac, James Kopczyk, and Travis Nuyens. *Photonic Sensors* (2012) Vol. 2, No. 3: 215–224.

[9] Reliability, durability and packaging of fibre Bragg gratings for large-scale structural health monitoring of defence platforms Davis, C., Grabovac, I., Kopczyk, J., Lombardo, P., Norman, P., Rizk, A., Nuyens, T.& Tejedor, S. (2013), *DSTO Technical Note*,DSTO-TN-2880.

[10] Low-temperature film adhesives for broad area application of distributed fibre optic strain sensors. Claire Davis, Patrick Norman, Peter Lombardo and Steve Galea. (2015), *DSTO Technical Note, DSTO-TN-1432*.

Appendix A: Materials Data Sheet Redux 312

Redux® 312

Modified epoxy film adhesive

Product Data

Description

Redux® 312 is a high strength 250°F curing film adhesive, suitable for metal to metal bonding and sandwich constructions, where operating temperatures of up to 212°F may be experienced.

A supported version, Redux® 312/5, is available with a woven nylon carrier for bond line thickness control.

Features

- Short cure cycle - cures in 30 minutes at 250°F
- Good mechanical performance up to 212°F
- Suitable for composite to composite bonding
- Low volatile content (solventless process)

Applications

- Metal to metal bonding
- Sandwich constructions
- Composite to composite bonding

Forms

Grey flexible film adhesive, available in 5 areal weights; 4 in unsupported form and one with a woven nylon carrier.

Product Description	Areal Weights psf	Roll Width in.	Standard Roll ft²
Redux® 312	0.015	21	645
Redux® 312UL	0.02	21	645
Redux® 312L	0.03	21	645
Redux® 312	0.06	21	645
Redux® 312/5	0.06	21	645

Instructions For Use

Pretreatment

It is essential that all substrates to be used are free of contamination and are in as ideal a state for bonding as possible. As pretreatment varies significantly depending on the substrates used, please refer to the Hexcel publication Redux® Bonding Technology for optimum procedures.

If there is to be a delay between the pretreatment and bonding of aluminium, the pretreated surface should be protected with Redux® 112 surface pretreatment protection solution to conserve the optimum bonding surface. This will enable bonding to be delayed for up to 2 weeks without deterioration of the pretreated surface. The correct application of Redux® 112 should not alter the bonding performance of Redux® 312 (for full application details consult the relevant data sheet).

HEXCEL

DISTRIBUTION LIST

Measurement of Surface Strains from a Composite Hydrofoil using
Fibre Bragg Grating Sensing Arrays

Claire Davis, Patrick Norman, Andrew Phillips and Asintha Nanayakkara

Task Sponsor

Dr. Ken Anderson CAD

S&T Program

Navy Scientific Adviser
Research Leader (AHS): Dr Peter Frith
Science Team Leader: Dr Claire Davis
Head of Group: Dr Steve Galea
Chief Maritime Division: Dr Janis Cocking
SEA 1000 S&T Advisor: Mr Kevin Gaylor
Research Leader Undersea Command and Control: Dr David Kershaw
Research Leader Sonar Technology and Systems: Dr David Liebing
Research Leader Maritime Autonomy: Dr Bryan Jessup
Research Leader Non- Acoustic Signature Management
Mr Leo de Yong
Research Leader Acoustic Signature Management: Dr Chris Norwood
Research Leader Naval Architecture: Dr Stuart Cannon
Group Leader – Hydroacoustics: Mr Brendon Anderson
Group Leader- Environmental Signature Control: Ms Lyn Fletcher
Group Leader – Platform Systems Analysis and Performance:
Mr Andrew Tynan
SEA 1000 Adelaide - Technology and Operational Analysis Liaison: Dr Robert
O'Dowd
Staff Officer Science SEA 1000: Mr Ross Susic
DST SEA 1000 Project Coordinator: Ms Carol Batras

Navy

Deputy Director Submarine Capability – Acquisitions: CDRE Peter Scott
Director General Technical Seaworthiness: CMDR Rodney Horsburgh

Defence Materiel Organisation

Head Future Submarine Program: RADM Greg Sammut
Director General Future Submarine Program: CDRE Michael Houghton
Director of Engineering Future Submarine Program: Mr David Simcoe

Director Future Submarine Program Logistics: CAPT Chris Roberts
Submarine Program Chief of Staff: Mr Bob Clark

Principal Mechanical Engineer – Directorate of Submarine Engineering:
Mr Andrew Gates

Future Submarine Program – Adelaide Office

Power and Propulsion Manager: Mr Maurizio Di Lorenzo

Naval Surface Warfare Center – USA

Advanced Material Propeller – Program Manager: Dr Scott Black

DEFENCE SCIENCE AND TECHNOLOGY ORGANISATION DOCUMENT CONTROL DATA		1. DLM/CAVEAT (OF DOCUMENT)

2. TITLE Measurement of Surface Strains from a Composite Hydrofoil using Fibre Bragg Grating Sensing Arrays	3. SECURITY CLASSIFICATION (FOR UNCLASSIFIED REPORTS THAT ARE LIMITED RELEASE USE (L) NEXT TO DOCUMENT CLASSIFICATION) Document (U) Title (U) Abstract (U)

4. AUTHOR(S) Claire Davis, Patrick Norman, Andrew Phillips and Asintha Nanayakkara	5. CORPORATE AUTHOR Defence Science and Technology Group 506 Lorimer St Fishermans Bend Victoria 3207 Australia

6a. NUMBER DST-Group-TN-1438	6b. AR NUMBER AR-016-356	6c. TYPE OF REPORT Technical Report	7. DOCUMENT DATE July 2015

8. FILE NUMBER	9. TASK NUMBER	10. TASK SPONSOR	11. NO. OF PAGES 33	12. NO. OF REFERENCES 10

13. Publications Repository http://dspace.dsto.defence.gov.au/dspace/	14. RELEASE AUTHORITY Chief, Aerospace Division

15. SECONDARY RELEASE STATEMENT OF THIS DOCUMENT

Approved for public release

OVERSEAS ENQUIRIES OUTSIDE STATED LIMITATIONS SHOULD BE REFERRED THROUGH DOCUMENT EXCHANGE, PO BOX 1500, EDINBURGH, SA 5111

16. DELIBERATE ANNOUNCEMENT

No Limitations

17. CITATION IN OTHER DOCUMENTS	Yes

18. RESEARCH LIBRARY THESAURUS

fibre Bragg grating, fibre optic strain gauge, composite hydrofoil

19. ABSTRACT

This report details a methodology for the permanent attachment of fibre optic strain gauge (Bragg grating) arrays to the surface of a composite hydrofoil and reports on an experiment to measure surface strains from the hydrofoil under static and fatigue loading conditions. The strain data from the optical gauges is compared to measurements from electrical resistance strain gauges nearby and to model predictions and an assessment is made on the suitability of this technique for strain-mapping in a service environment.